1962

An investigation of the deformation textures of cobalt

Roy Carl Wilcox

AN INVESTIGATION OF THE DEFORMATION TEXTURES OF COBALT

An Abstract of a Dissertation

Presented to

the Faculty of the Graduate School

University of Missouri

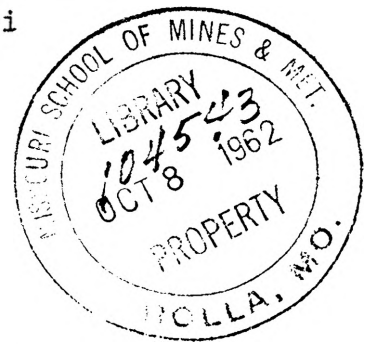

In Partial Fulfillment

of the Requirements for the Degree

Doctor of Philosophy

---

by

Roy Carl Wilcox

March 1962

AN INVESTIGATION OF THE DEFORMATION TEXTURES OF COBALT

Deformation textures of various cobalt structures as a result of cold rolling together with some annealing textures were studied. The textures of cobalt were determined using a modification of the Schulz-Decker Geiger counter technique. Pole figures of the $(10\bar{1}1)$, (0001) and $(10\bar{1}0)$ planes were constructed. Also, a study of the microhardness of cobalt was made.

Microhardness tests were performed on various cobalt structures, in both the cold rolled and unworked conditions. The microhardness was found to vary with the source of the cobalt, the crystal orientation, and the amount of deformation and twinning. Deformation lines about the hardness impressions diffused and became broader with time, indicating that partial self-relief of the imposed stress may take place.

Textures of electrodeposited cobalt in (1) the as-deposited condition; (2) cold rolled eight percent without an initial anneal; and (3) cold rolled twenty percent with an initial anneal above the allotropic transformation were studied. Electrodeposited cobalt was found to have mainly a $[10\bar{1}0]$ texture with a large spread toward a $[11\bar{2}0]$ texture. The texture of the deposited cobalt with eight percent reduction by rolling was unchanged from the original texture. However, twenty percent reduction by rolling after annealing

above the allotropic transformation produced a (0001) $\langle 11\bar{2}0 \rangle$ texture with partial retention of the original $[10\bar{1}0]$ texture. The texture of the "as-deposited" cobalt could not be completely destroyed by heat treatment.

Cold-rolled textures of sintered cobalt powders and annealed sponge were determined. The textures of both were practically the same. The texture can be described as (0001) $\langle 11\bar{2}0 \rangle$ in which the (0001) planes are rotated twenty to twenty-five degrees in the rolling direction from the rolling plane normal with the $\langle 11\bar{2}0 \rangle$ directions rotated twenty to twenty-five degrees in the transverse direction. The textures obtained are representative of cobalt textures up to approximately fifty or sixty percent reduction.

The deformation textures of cobalt were examined theoretically by the Calnan and Clews method of texture analysis. From these theoretical considerations, the deformation mechanisms occuring during cold rolling of cobalt were determined to be (0001) $[11\bar{2}0]$ slip and $\{10\bar{1}2\}$ twinning. A study of these deformation mechanisms in tension and compression allowed a theoretical (0001) pole figure to be constructed. The construction of this pole figure was made from considerations of the rotations involved in tension and compression during deformation.

Annealing textures of rolled electrodeposited cobalt were also studied. The temperatures used were 385°F and 720°F, the latter being above the recrystallization range

but below the allotropic transformation. The textures resulting from the annealed rolled "as-deposited" cobalt are not representative of annealing textures because of the partial retention of the "as-deposited" texture throughout all the physical operations performed on the material.

ACKNOWLEDGMENTS

Appreciation is expressed to the people who helped to make this thesis possible, in particular, to Dr. D. S. Eppelsheimer, Professor of Metallurgical Engineering, for his supervision and assistance during the course of the investigation, and Dr. T. J. Planje, Professor of Ceramic Engineering, for his advice and assistance during the X-ray examination.

The author would like to thank G. A. Fisher of the International Nickel Company and J. A. Lund of the University of British Columbia for furnishing the cobalt materials used in this investigation. Thanks is also expressed to F. R. Morral of the Cobalt Information Center, Battelle Memorial Institute for his assistance in obtaining the samples used.

Also, the author would like to thank Dr. J. F. Eckel Head, Department of Metallurgical Engineering at Virginia Polytechnic Institute and all the others who were responsible for the author's leave of absence from the above school.

AN INVESTIGATION OF THE DEFORMATION TEXTURES OF COBALT

A Dissertation

Presented to

the Faculty of the Graduate School

University of Missouri

In Partial Fulfillment

of the Requirements for the Degree

Doctor of Philosophy

---

by

Roy Carl Wilcox

March 1962

TABLE OF CONTENTS

CHAPTER PAGE

CHAPTER PAGE

CHAPTER PAGE

LIST OF TABLES

TABLE PAGE

LIST OF FIGURES

FIGURE PAGE

FIGURE PAGE

FIGURE PAGE

FIGURE PAGE

CHAPTER I

INTRODUCTION

Because cobalt is chemically very similar to nickel, only within the last few years has it been possible to produce high-purity cobalt. For this reason, the mechanical properties of pure cobalt are not well known. As the purity of cobalt has increased, research has been undertaken to enlarge the knowledge of the properties of cobalt. However, even in recent years, most cobalt research has been centered about the production of high-purity cobalt or the allotropic transformation and its mechanisms. The study of the allotropic transformation has been continuous for the past forty years, and still the transformation is not fully understood because of its martensitic nature. Although uses of cobalt are confined mostly to cobalt-containing alloys or cobalt tool alloys, much interest in the properties of pure cobalt has been generated by the Cobalt Information Center at Battelle Memorial Institute, Columbus, Ohio.

For the past ten years, the Department of Metallurgy of the Missouri School of Mines and Metallurgy, Rolla, Missouri has been interested in deformation textures and mechanisms of the hexagonal metals. To date, only hafnium and titanium have been investigated at the Missouri School of Mines, and the study of cobalt is a continuation of this interest in hexagonal metals. Zinc, magnesium, zirconium,

and beryllium have been studied elsewhere. It is felt that after a sufficient number of hexagonal metals have been investigated, a general theory of deformation may be proposed for them.

The problem of deriving a satisfactory theory for the deformation of hexagonal metals is difficult because of the differences in the c/a ratios of these metals. Hexagonal metals can be classified into three groups according to the c/a ratio: (1) those metals with a c/a ratio greater than 1.633; (2) those metals with a c/a ratio approximating the ideal ratio of 1.633; and (3) those metals with a c/a ratio less than 1.633. Zinc is an example of the first group; magnesium and cobalt, the second; and hafnium, zirconium, titanium, and beryllium, the third. Each group of hexagonal metals has a different deformation texture and deformation mechanism from the other two groups and may differ also within the same group. Thus, comparison between the various hexagonal metals is difficult.

To reduce the confusion concerning the deformation of hexagonal metals, this study was undertaken: (1) to determine the texture developed in cobalt as a result of deformation; (2) to determine the effect of annealing on the deformation textures; (3) to develop an explanation of the deformation mechanisms involved in producing the observed deformation textures of cobalt; and (4) to determine the reasons for the

differences between the observed texture of cobalt and the texture of magnesium which has the closest c/a ratio to cobalt. Even though much work has been done on cobalt, a search of the literature revealed that little effort had been made to determine experimentally the deformation textures of cobalt. It is hoped therefore, that this investigation will extend the knowledge of cobalt and other hexagonal metals.

CHAPTER II

REVIEW OF THE LITERATURE

A. PHYSICAL PROPERTIES OF COBALT

Cobalt, atomic number 27, is in Group VIII, between iron and nickel, toward the end of the transition elements of the first long period of the Periodic Table of the Elements. The electron configuration of cobalt outside the argon structure is $3d^7$, $4s^2$. The incomplete 3d level accounts for its ferromagnetism. The chemical valence can be either two or three, but in alloying the valence is considered to be zero when forming solid solutions.

Cobalt has advanced from being just a glass coloring agent in 2500 B.C. to that of great metallurgical industrial importance today. (1) The uses of cobalt include among others, magnetic alloys, high-temperature alloys, and high-speed tool-steel alloys.

Cobalt has a hexagonal close-packed structure at room temperature, with a space group of C6/mmc in the Hermann and Mauguin system. The lattice parameters (2) are:

$a = 2.5071$ Å

---

(1) F.R. Morral, Chronology of Cobalt, (Columbus: Battelle Memorial Institute, 1958).

(2) R.T. Anantharaman, "Lattice Parameters and Crystallographic Angles of Hexagonal Cobalt," Current Science, Vol. 27, pp. 51-53, 1958.

$c = 4.0686$ Å

$c/a = 1.6228$

At 417°C the hexagonal close-packed structure transforms to a face-centered cubic structure with a room temperature lattice parameter of 3.56 Å. The hexagonal structure contains two atoms per unit cell while the cubic structure contains four atoms per unit cell. (3)

The allotropic transformation has been studied for many years. An X-ray pattern of cobalt, (4) instead of showing just the hexagonal lines or the cubic lines, shows lines of both structures because the face-centered cubic to hexagonal close-packed transformation is sluggish and the high-temperature structure (f.c.c.) is retained at room temperature. However, lines which are common to both structures are sharp and the lines which are not common to both structures are diffuse and sometimes very weak. This effect may be explained by a lattice structure which has layers stacked in the hexagonal close-packed arrangement alternating in random manner with layers stacked in the cubic close packing.

The crystallographic angles between sets of planes in

---

(3) F.R. Morral, Cobalt and Its Alloys, (Columbus: Stoneman Press, 1958), p. 7.

(4) H.P. Klug and L.E. Alexandria, X-Ray Diffraction Procedures, (New York: John Wiley and Sons, 1954), p. 385.

face-centered cubic cobalt can be calculated from lattice geometry or found in prepared tables of inclination angles between plane normals in cubic crystals such as found in Structure of Metals by Barrett. (5) However, for hexagonal close-packed cobalt, the crystallographic angles must be calculated because the angles depend on the c/a ratio which differs for each hexagonal structure. These angles can be calculated by the following expression: (6)

$$\text{Cos } \phi = \frac{h_1h_2+k_1k_2+\frac{1}{2}(h_1k_2 + h_2k_1) + 3/4\,(\frac{a}{c})^2\, l_1l_2}{\sqrt{(h_1^2+k_1^2+h_1k_1+3/4(\frac{a}{c})^2l_1^2)\,(h_2^2+k_2^2+h_2k_2+3/4(\frac{a}{c})^2l_2^2)}} \qquad (1)$$

Where the ϕ is the angle between the normals to the plane $(h_1k_1l_1)$ and the plane $(h_2k_2l_2)$, and where a and c are lattice constants. These calculations have been performed for many crystallographic angles in relation to the (0001) and (1010) planes in cobalt by Anantharaman. (7)

B. TEXTURES

Normally, each grain in an aggregate has a crystallographic orientation which is different from that of its

---

(5) C.S. Barrett, Structure of Metals, (New York: McGraw-Hill Book Company, 1952), p. 36.

(6) L.G. Morell and J.D. Hanawalt, "X-Ray Study of Plastic Working of Magnesium Alloy," Journal of Applied Physics, Vol. 7, p. 163, 1932.

(7) Anantharaman, Loc. cit.

neighbors. Therefore, the orientation of all the grains in an aggregate may be random to some reference point or may tend to group about some particular orientation. This is known as preferred orientation or texture. (8)

Crystals in a cold-drawn wire are oriented in such a manner that the same crystallographic direction in most of the grains is parallel or nearly so to the wire or fiber axis. (9) In cold-rolled sheet most of the grains are oriented so that a certain direction in that plane is parallel to the sheet surface, and a certain direction in that plane is parallel to the direction of rolling. (10) These deformation textures are due to the tendency of the slip planes to rotate during plastic deformation.

Preferred orientation is a crystallographic condition only and has nothing to do with the microscopic grain shape. Therefore, only X-ray diffraction can give evidence of preferred orientation. (11)

In material with a fiber texture, (12) the grains have a common crystallographic direction parallel to the fiber axis, but they can have any rotational position about the axis. The textures of rolled sheet differs from that of wire in having less symmetry. There is no common crystallographic

---

(8) B.D. Cullity, Elements of X-Ray Diffraction, (Reading, Mass.: Addison-Wesley, 1956), pp. 272-274.

(9) Ibid. (10) Ibid. (11) Ibid. (12) Ibid. p. 280.

direction about which the grains can have any rotational position.

Barrett (13) states that, in general, the principal orientation for cold-rolled face-centered cubic metals is the (11C) set of planes parallel to the rolling plane and the [112] direction parallel to the rolling direction, giving a (110) [112] texture. There is sometimes a secondary orientation present in the f.c.c. metals, the (112) [111] .

Rolling should tend to rotate the slip planes of hexagonal close-packed metals into the plane of the rolled sheet. (14) Thus, the predominating texture is one in which the basal plane (slip plane) lies in or near the rolling plane. This texture is most pronounced in metals with an axial ratio near that for the close packing of spheres (c/a = 1.633), such as in magnesium, zirconium, and cobalt. In magnesium there is a tendency for the [11$\bar{2}$0] direction to align with the rolling direction.

C. X-RAY TECHNIQUE

The technique used for the determination of preferred orientation in metals is the construction of pole figures. (15)

---

(13) C.S. Barrett, Structure of Metals, (New York: McGraw-Hill Book Company, 1952), p. 457.

(14) Ibid., p. 473.

(15) H.P. Klug and L.E. Alexander, X-Ray Diffraction Procedures, (New York: John Wiley and Sons, 1954), p. 573.

A pole figure, which is a stereographic plot of the poles of a reflecting plane, provides a relatively complete picture of the nature and perfection of the orientation. For perfect orientation, the plot of the poles on the stereographic projection is shown as points. These points spread out into areas on the projection with any deviation from the perfect orientation. Thus, the pole figure clearly presents the extent of variation from the ideal orientation. The construction of a pole figure therefore requires some means of determining the diffracted intensity of a reflecting plane through all possible angles of rotation. A series of X-ray photographs or a Geiger counter X-ray spectrometer are usually the means by which the areas of the poles are determined.

Preparation of Samples. The factors which determine the choice of specimens and the method of preparation vary with the specimen and the X-ray technique. (16) If the X-ray beam is to be passed through the specimen, the sample should be very thin to decrease the absorption of X-rays by the specimen. The thickness of cobalt samples would have to be less than 0.003 inches (Chapter V) to eliminate the absorption correction.

---

(16) A. Hargreave, "Methods of Examining Orientation Textures", X-Ray Diffraction by Polycrystalline Materials, (Long: The Institute of Physics, 1955), pp. 298-99.

For rolled-metal sheet, the specimen is usually cut from the original material and reduced to the required thickness by several methods. The thickness may be reduced by grinding and filing, but in this case, great care is required to prevent a great deal of deformation which might overshadow the effects of rolling. The surface layers of the material are deformed by grinding and must be removed by etching. When possible, this technique should be avoided. The best method is to reduce the size completely by etching.

A plate specimen may also be prepared in the shape of a cylindrical rod instead of a flat sheet (17) for photographic studies. This method eliminates corrections for absorption of the X-ray beam by the specimen. The rod specimens are prepared by cutting a small plate from the sheet with the length parallel to the cylinder axis, the cylinder axis being the direction of rolling. The plate is then reduced by grinding until the cross-section is square and then circular. The specimen is then etched to remove the effect of the deformation caused by grinding.

Wire and electrodeposited metal specimens may be prepared for X-ray examination by using methods similar to those described for rolled-metal sheet. (18)

---

(17) P. W. Bakarian, "Preferred Orientation in Rolled Magnesium and Magnesium Alloys", Transactions AIME, Vol. 147, pp. 267, 1942.

(18) Hargreave, Loc. cit.

Diffractometer Method for Pole Figures. Decker (19) and Schulz (20) derived methods of determining pole figures with the use of a Geiger counter X-ray diffraction spectrometer. These methods are capable of high precision because the intensity of the diffracted rays is measured quantitatively with a Geiger counter, and the intensity measurements are corrected for changes in absorption and defocusing.

Decker's method (21) involves transmission studies of a very thin sample. A special specimen holder is required which allows rotation of the specimen about the diffractometer axis and about a horizontal axis normal to the specimen surface. These rotations move the pole of the reflecting plane over the surface of the pole figure, which is plotted on a projection plane parallel to the specimen plane. At each position of the specimen, the measured intensity of the diffracted beam after correction for absorption gives a figure which is proportional to the pole density at the corresponding point on the pole figure.

---

(19) B.F. Decker, E.T. Asp, and D. Hacker, "Preferred Orientation Determinations Using a Geiger Counter X-Ray Diffraction Goniometer", Journal of Applied Physics, Vol. 19, p. 388, 1948.

(20) L.G. Schulz, "A Direct Method of Determining Preferred Orientation in Flat Reflection Samples Using a Geiger Counter X-Ray Spectrometer", Journal of Applied Physics, Vol. 20, p. 1030, 1949.

(21) Decker, Loc. cit.

An absorption correction is necessary in this method because variations in the angles about the diffractometer axis causes variations in both the volume of diffracting material and the path length of the X-rays within the specimen. Variations of the angles of rotation of the specimen within its own plane have no effect. Thus, the factor for changing observed intensity to corrected intensity is

$$I_o/I_{\pm\alpha} = \frac{\mu t \exp[-\mu t/\cos\theta]}{\cos\theta} \times \frac{\cos(\theta\pm\alpha)/\cos(\theta\mp\alpha) - 1}{\exp[-\mu t/\cos(\theta\pm\alpha)] - \exp[-\mu t/\cos(\theta\mp\alpha)]} \qquad (2)$$

where I_o is the observed intensity; $I_{\pm\alpha}$ is the corrected intensity; μ, the linear absorption coefficient; t, the specimen thickness; α, the angle of rotation; and θ is the Bragg angle of the reflecting plane. Each observed intensity at a given angle of α is multiplied by the correction factor for that angle and the corrected intensities are used for plotting the pole figure. However, the central part of the pole figure cannot be covered by this transmission method.

The value of μt in the above equation must be obtained by direct measurement, because it is not sufficiently accurate to use a tabulated value of μ together with the measured thickness of the specimen. The measurement of the intensity of a strongly diffracted beam from any convenient material when the sample is inserted in the diffracted beam and again when it is not serves to determine μt. The value of μt is

then obtained from the general absorption equation,

$$I_t = I_o \exp(-\mu t) \qquad (3)$$

where I_o and I_t are the intensities without and with the sample in the diffracted beam, respectively.

Schulz' (22) method involves reflection in which the measured diffracted beam issues from the same side of the specimen on which the primary beam is incident. The reflection method also requires a special holder which allows rotation of the specimen in its own plane about an axis normal to its surface and about a horizontal axis. This method explores the central part of the pole figure which is not covered by the Decker method. The great virtue of the reflection method is that no absorption correction is required for values of revolution between -90° and about -40°. However, the intensity of the diffracted beam must be corrected for defocusing of the sample as the specimen is rotated about the diffractometer axis. The corrected intensities are proportional to the pole density.

In 1952, Williams (23) (24) constructed a universal

---

(22) Schulz, Loc. cit.

(23) D.N. Williams, "An Investigation of the Deformation Texture of Titanium", University of Missouri, Ph.D. Disseration, (MSM-T1036) 1952.

(24) D.N. Williams and D.S. Eppelsheimer, "Universal Specimen Mount for Pole Figure Determination Using the Schulz-Decker Technique", Missouri School of Mines

specimen mount which incorporates the best features of both Decker and Schulz. With this type of mount the transmission and reflection methods complement each other to cover the entire pole figure. (25) The transmission method is used to cover the pole figure from 0° to -30° and the reflection from -30° to -90°. This produces an overlap which is necessary in order to find a normalizing factor for one set of readings and make them agree with the other set in the region of overlap.

When this is done, the numbers which are proportional to pole density can be plotted on the pole figure at each point at which a measurement was made. Contour lines are then drawn at selected levels connecting points of the same pole density. Such a pole figure is more accurate than one determined photographically and represents the best representation of the kind and extent of preferred orientation.

Defocusing Errors. Two defocusing errors are present when using the X-ray reflection method in determining pole figures. (26) The first defocusing error results when the

---

Technical Bulletin, No. 79, January, 1952.

(25) B.D. Cullity, Elements of X-Ray Diffraction, (Reading, Mass.: Addison-Wesley, 1956), pp. 292-293.

(26) W.P. Chernock and P.A. Beck, "Analysis of Certain Errors in the X-Ray Reflection Method for the Quantitative Determination of Preferred Orientation", Journal of Applied Physics, Vol. 23, pp. 341-345, 1952.

specimen is rotated about the diffractometer axis, and certain parts of the irradiated area of the specimen move off the focusing circle described by the source, the specimen surface, and the receiving slit. This has the effect of reducing the recorded intensity of even a completely random oriented powder as the angle of revolution increases from the center of the polar net. This effect can be minimized by keeping the width of the pole figure fixture slits as narrow as possible while retaining sufficient diffraction intensity and widening the receiving slits as much as is practicable. This last factor will result in a decrease in angular revolution, and in some cases, in insufficient separation of reflections from different crystal planes. The best method to minimize this defocusing error is to run a completely random oriented powder through all angles of revolutions and calculate the factor necessary to bring the recorded intensities at all angles back to the original intensity at the center of the polar net. These factors are then multiplied by the intensities recorded from oriented material to prevent this defocusing from being superimposed on the pole figure.

The second defocusing effect is due to misalignment of the specimen during mounting. This will result in a movement of the diffraction peaks from the correct 2θ values and cause a decrease in intensity. The maximum allowable misalignment is a variation of 0.05° in 2θ between $\phi = 0$ to

$\phi = 45^{\circ}$ clockwise and to $\phi = 45^{\circ}$ counter-clockwise, where ϕ is the angle of revolution. The only way to minimize this error is to properly align the specimen.

CHAPTER III

COMPOSITION AND PREPARATION OF SAMPLES

A. HISTORY AND COMPOSITION

Electrodeposited Sheet. The electrodeposited cobalt used in this investigation was furnished by the International Nickel Company. The "as-received" material was in the form of electrodeposited sheets, 0.04 to 0.07 inches in thickness. The composition of these sheets is given in Table I.

Rolled Powder. The wrought powdered cobalt was furnished by the University of British Columbia. All samples were prepared from sintered powders and fabricated from the same batch of cobalt powder. The chemical analysis of the powders is given in Table I and the physical history of the samples is given below:

Processing of the strips:

1. Roll compacting
2. Sintered 4 hrs. at 1150°C in cracked NH_3
3. Cold rolling 30%
4. Sintering 50 minutes at 1150°C (cracked NH_3)
5. Cold rolling 20%
6. Annealing 15 minutes at 980°C (cracked NH_3)
7. Cold rolling 20%
8. Annealed 15 minutes at 980°C (cracked NH_3)
   a. cold rolling 15%
   b. cold rolling 10%
   c. cold rolling 5%

Annealed Sponge. The "annealed sponge" used in this investigation was produced from vacuum melted ($< 0.5\mu$)

TABLE I

COMPOSITION OF COBALT SAMPLES

Element	Percent		
	Electro-deposited	Powder	Sponge
Ni	0.45	0.08	0.0005
C	0.01-.02	0.052	
Fe	0.001	0.007	0.009
S	0.001	0.032	
Pb	0.0001		
Zn	Trace		
As	Trace		
Bi	Nil		
Cu		0.002	
Si			<0.0001
Mg			0.0001
Na			0.0001
Ca			0.0001
Cr			<0.0001
Mo			0.09-.22
Zr			<0.001
W			<0.001

Johnson-Matthey sponge. The cast sponge was hot-forged and hot-rolled. The hot rolling reduced the thickness from 0.39 to 0.05 inches. After hot working, the wrought sponge was annealed at 1176°C, which is 759°C above the allotropic transformation temperature. After annealing, the material was pickled in 20 percent HCl. This stock will be referred to as annealed sponge or sponge in the discussion of this investigation. The composition of the sponge is given in Table I.

B. COLD ROLLING

Preparation of Samples. The "as-received" material was cut and ground carefully to give a rectangular shape to the samples. After shaping, the samples were etched with concentrated HCl to remove any grit or oxide which may have been present on the surface.

The thickness of each sample after etching was measured, and this thickness was used in the calculation of the percent reduction during rolling. The percent reduction in thickness as a result of rolling was used to determine the amount of deformation. The samples before rolling were approximately 2.5 centimeters long, 1.5 centimeters wide and from 0.15 to 0.25 centimeters thick.

Cold Rolling of Samples. A set of six-inch laboratory rolls was used to prepare the cold-rolled specimens. Two-inch

rolls with a four-high mill were not used because the specimens had a tendency to bow during rolling and the radius of curvature of the bow was less using a two-high mill with six-inch rolls. The samples were rolled in one direction only but were turned 180 degrees between each pass. The samples were set aside between each pass to allow time for cooling to prevent any effect of temperature due to heat from mechanical deformation.

Table II shows the changes in thickness of a sample during rolling of "as-received" electrodeposited cobalt. The results of Table II illustrate that a large reduction is not possible. One large crack through the center of the specimen occurred at 8.5 percent reduction and broke into seven pieces with eleven percent reduction. With this sample, it is seen that approximately seven percent reduction is the maximum that can be obtained. In Figure 1, a photograph of the cold-rolled sample used for the data of Table II is shown. The large central crack formed with 8.5 percent reduction can be seen in the large piece. The small fragments produced with eleven percent reduction are also shown.

Even though the maximum safe reduction is approximately seven percent, eight percent reduction was obtained by very careful rolling with very small reductions with each pass. Small macroscopic cracks formed with about seven percent reduction but did not increase too much with further reduction to eight percent. When these macroscopic cracks became

TABLE II

CHANGES IN THICKNESS OF ELECTRODEPOSITED COBALT DURING 11 PERCENT REDUCTION

Thickness (in.)	No. of Passes	Percent Reduction
0.0590	0	0
0.0575	3	2.5
0.0563	4	4.7
0.0550	5	6.8
0.0540	6	8.5 (cracked)
0.0525	7	11.0

Figure 1. Electrodeposited Cobalt Reduced 11 Percent by Cold Rolling. 2X.

visible to the eye in the majority of the maximum reduced specimens, the rolling was ceased, and this amount of reduction was used as the maximum percent reduction. The majority of these cracks were formed in the center and at the ends of the specimen and not at the edges. The data in Table III are taken from the eight percent reduced electrodeposited sample.

The cold rolling of the vacuum melted and annealed sponge and the annealed electrodeposited cobalt was carried out in the same manner as the electrodeposited cobalt without annealing. However, the maximum amount of reduction with the annealed electrodeposited cobalt was twenty percent while for the annealed sponge, the maximum reduction was forty percent before macroscopic cracks became harmful. Table IV gives the changes in thickness of the forty percent cold-rolled sponge sample during rolling. The percent reductions shown in Table IV were obtained by the use of the following equation:

$$R = \frac{T_O - T_R \times 100}{T_O}$$

where R is the percent reduction, T_O is the original thickness, and T_R is the thickness after rolling.

C. ANNEALING

Preparation of Samples. The samples to be annealed were etched with concentrated HCl to remove any grit or oxide which may have been present on the surface. After etching,

TABLE III

CHANGES IN THICKNESS OF ELECTRODEPOSITED COBALT DURING 8 PERCENT REDUCTION

Thickness (in.)	No. of Passes	Percent Reduction
0.0805	0	0
0.0798	4	1.0
0.0780	8	3.0
0.0755	12	4.2
0.0740	16	8.0

TABLE IV

CHANGES IN THICKNESS OF ANNEALED COBALT SPONGE DURING 40 PERCENT REDUCTION

Thickness (in.)	No. of Passes	Percent Reduction
0.043	0	0
0.040	4	7.0
0.036	8	16.3
0.029	12	32.5
0.026	14	40.0

each sample was vacuum sealed in a pyrex tube. The pyrex tubes also contained chips of a titanium-zirconium alloy which were used as a deoxidizer. The sealing in the pyrex tubes was done to prevent oxidation during the annealing process.

Annealing of Samples. The pyrex tubes containing the annealing samples were inserted in a pre-heated pot-furnace at one of three temperatures; 385°F, 720°F, and 840°F. All the electrodeposited cobalt samples which were to be rolled to reductions greater than ten percent were heat-treated at 840°F for 100 hours before rolling. This temperature is above the transformation temperature, and thus destroyed some but not all of the electrodeposited texture, enabling a greater amount of reduction than on the "as-received" material.

After the initial annealing at 840°F, the samples were rolled to the desired reduction and resealed in pyrex tubes for further heat treatment. The heat treatment consisted of one hour at one of the before mentioned temperatures. Samples were heat-treated and furnace-cooled at 385°F and 720°F. Samples were also quenched in water from these temperatures. In addition, samples were annealed at 385°F, furnace-cooled and reannealed at 720°F and furnace-cooled. Also, the same procedure was carried out by quenching samples from each temperature. Table V lists all samples which were used in this work. Included is the heat treatment performed on each sample.

TABLE V

TREATMENT PERFORMED ON COBALT SAMPLES

Type	Annealing before Rolling	Amount of Reduction(%)	Heat Treatment after Rolling
Rolled Powder	None	5	None
	None	10	None
	None	15	None
Sponge	None	10	None
	None	20	None
	None	30	None
	None	40	None
Electro-deposited	None	as-received	None
	None	8	None
	100 hr 840°F	None	None
	100 hr 840°F	20	1 hr 385°F-FC*
	100 hr 840°F	20	1 hr 385°F-Q**
	100 hr 840°F	20	1 hr 720°F-FC
	100 hr 840°F	20	1 hr 720°F-Q
	100 hr 840°F	20	1 hr 385°F-FC 1 hr 720°F-FC
	100 hr 840°F	20	1 hr 385°F-Q 1 hr 720°F-Q

*FC - Furnace-cooled

**Q - Quenched

CHAPTER IV

METALLOGRAPHY OF COBALT

A. MICROSTRUCTURE OF COBALT

Because the grain size and crystal orientation of a metal have an effect on the amount of cold reduction obtainable in the metal and also on the final texture resulting from cold reduction, a microscopic examination of the cobalt used in this investigation was undertaken. All specimens were polished mechanically and either chemically or electrolytically etched (27) with 60 parts HCl, 15 parts HNO_3, and 15 parts H_2O. The techniques used for the preparation of the cobalt specimens for metallography are discussed in Appendix IV.

Electrodeposited. Metallographic examination of the electrodeposited cobalt was performed both normal and parallel to the direction of crystal growth during electrodeposition. Figures 2 and 3 show the microstructure normal and parallel to the direction of growth, respectively. From these photomicrographs, it is evident that the crystals are columnar. In the direction of growth the grains are very long without good grain boundary definition with respect to

---

(27) Metallographic Etching Reagents for Cobalt and Cobalt-Containing Alloys, (Columbus: Cobalt Information Center).

Figure 2. Microstructure of Electro-deposited Cobalt Parallel to Direction of Crystal Growth. 100X.

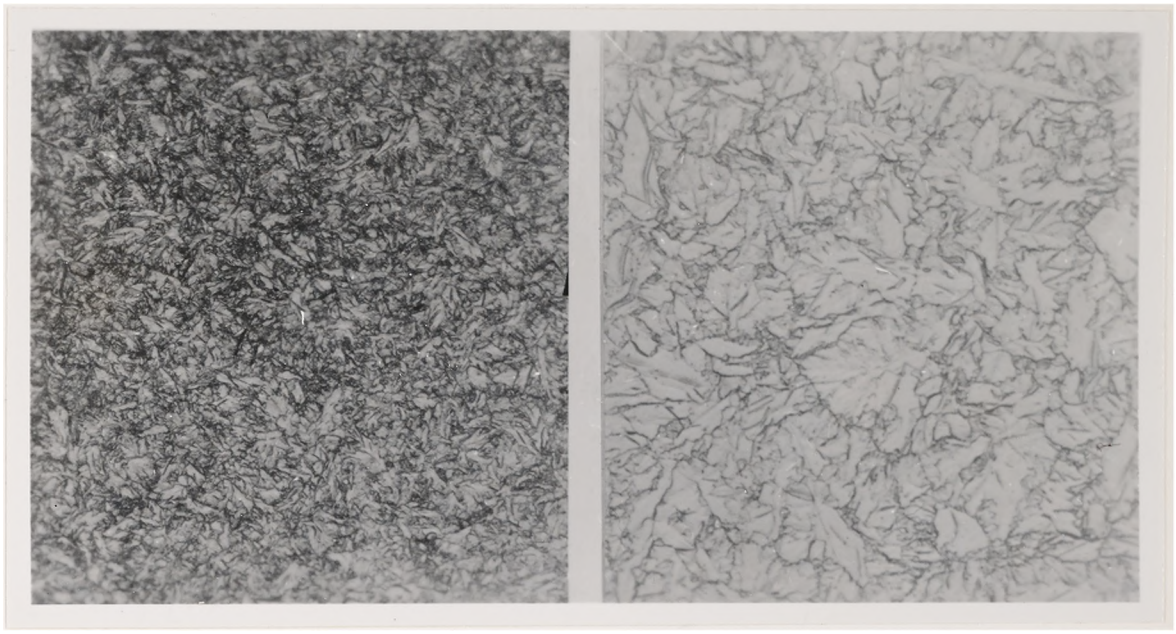

a b

Figure 3. Microstructure of Electrodeposited Cobalt Normal to Direction of Crystal Growth: (a) 100X; (b) 325X.

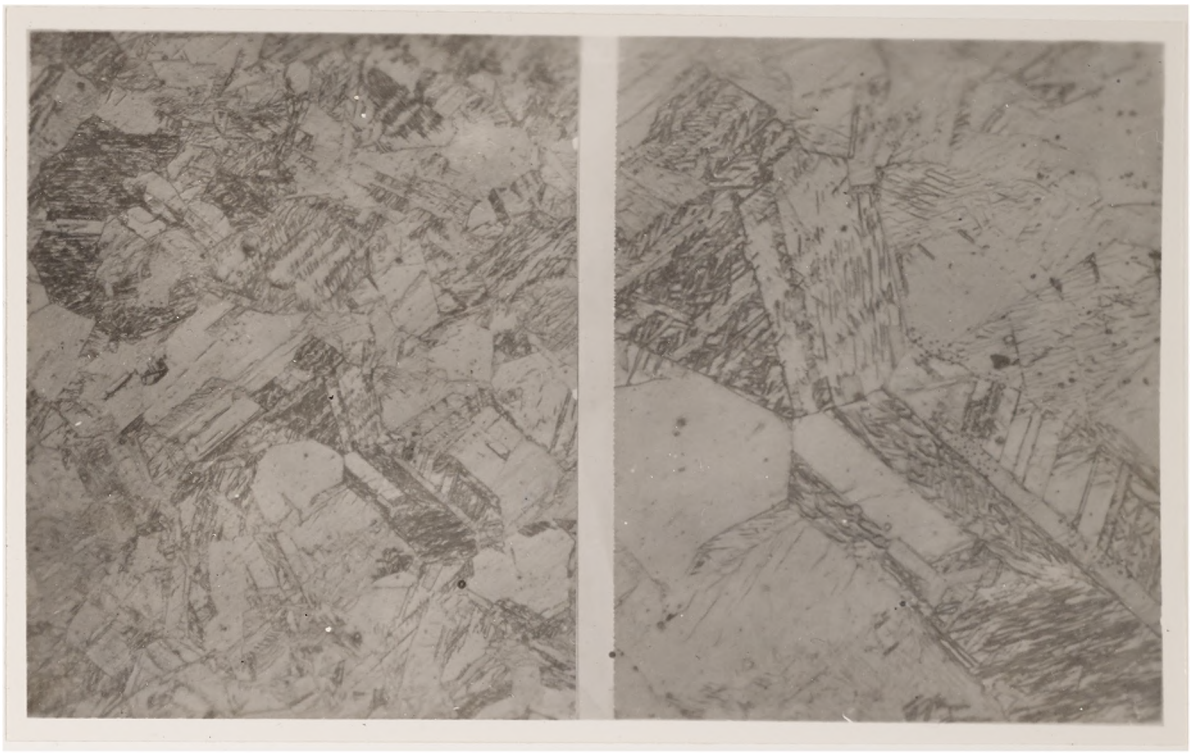

a b

Figure 4. Microstructure of Annealed Cobalt Sponge: (a) 100X; (b) 325X.

a b

Figure 5. Microstructure of Annealed Cobalt Sponge: (a) Cold Rolled 10 Percent; (b) Cold Rolled 40 Percent. 325X.

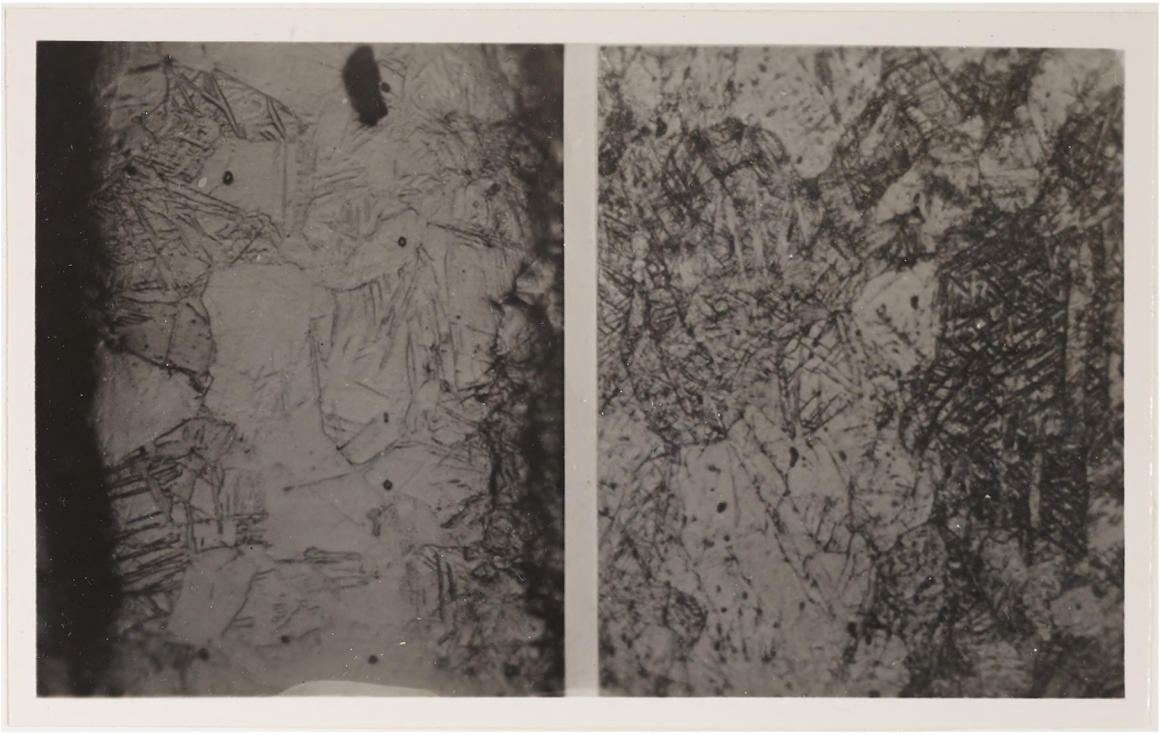

a b

Figure 6. Microstructure of Rolled Cobalt Powder: (a) Cold Rolled 5 Percent; (b) Cold Rolled 15 Percent. 325X.

the cross-section through the grains. This columnar growth and the texture associated with this growth proved to be a source of difficulty in the texture studies of the deformed electrodeposited cobalt.

Annealed Sponge. Figure 4 shows the microstructure of the "as-received" sponge, and Figure 5 shows the structure of the sponge after ten percent and forty percent cold rolling. A comparison of the "as-received" sponge with the electrodeposited cobalt reveals that the grain size of the sponge is much larger than that of the deposited cobalt transverse to the growth direction. This larger grain size of the sponge permitted greater reductions than possible in the deposited cobalt. Twinning as a result of the allotropic transformation is evident in the "as-received" sponge.

Elongation of the grains due to rolling is not too evident in the ten percent rolled structure, while it is fairly pronounced in the forty percent rolled structure. It is also quite evident that the amount of twinning as a result of deformation has increased with deformation.

Rolled Powder. Figure 6 shows the microstructure of five percent and fifteen percent cold-rolled sintered cobalt powder. Both photomicrographs are parallel to the rolling direction. The grain boundaries in the five percent rolled sample are more noticeable than those in the fifteen percent rolled sample due to the increased deformation in the latter.

The amount of twinning in the five percent rolled powder is relatively small with a large increase in twinning with fifteen percent rolling. Thus, as deformation increases, twinning increases which rotates new slip planes into position for slip. Without this twinning, the possible cold reduction of a hexagonal metal is very small.

B. MICROHARDNESS OF COBALT

Microhardness tests using a Bergsman Micro Hardness Tester were made on various cobalt structures. The cobalt samples consisted of the electrodeposited material, rolled powder, and sponge after hot rolling followed by annealing at 1176°C. The latter two types of samples had varying amounts of cold reduction by rolling.

All tests were conducted at room temperature, using a 100 gm load applied for twenty seconds. A 21X objective lens was used in the measurement of all indentations. The screw micrometer used for the measurement of the diagonals of the indentations was calibrated for the 21X objective lens against a stage micrometer graduated to 0.01 mm. The calibration for the above combination was 6064.4 units on the screw micrometer per 1 mm. All readings were converted to diamond pyramid hardness numbers by the following formula from the Metals Handbook: (28)

---

(28) Metals Handbook, 1948 Edition, (Cleveland: American Society for Metals, 1948), p. 92.

$$D.P.H. = \frac{1.8544\ L}{d^2}$$

where

D.P.H. = diamond pyramid hardness number
L = load in kilograms (4)
d = length of diagonals in mm.

Since the hardness indentations were of the order of 0.029 mm, a difference of one unit on the screw micrometer resulted in a change of 3 in the diamond pyramid hardness number. This is less than a 0.0002 mm change in the diagonals of the impression. Thus, a small error in reading the micrometer produced a large difference in the hardness.

Morral (29) reported that the room-temperature hardness of zone-refined cobalt varied from 81 to 249 BHN. He attributed this difference in hardness to differences in orientations of the indentations which were made within a given crystal. He also observed that the types of deformation resulting from the hardness tests were dependent upon the orientation of the indentations within a given crystal. He concluded that high hardness was associated with $\{11\bar{2}0\}$ twinning, and that low hardness was associated with extensive basal slip on the (0001) planes. These results have been partially confirmed by the tests reported in this paper.

---

(29) F.R. Morral, "High-Purity Cobalt..Its Properties", Journal of Metals, Vol. 10, pp. 662-664, 1958.

Electrodeposited Cobalt. Figure 7 shows the indentations made during the microhardness tests on electrodeposited cobalt. Figure 7a is normal to the direction of growth, while in Figure 7b it is parallel to the direction of growth of the grains during electrodeposition.

From the comparison of these photomicrographs, it is seen that the hardness indentations parallel to the growth (Figure 7a) are smaller than those normal to the direction of growth (Figure 7b). Thus, the hardness parallel to the growth is greater than normal to the growth. The DPH numbers for the indentations parallel to the growth are 216 and 210 from top to bottom in Figure 7a. For the indentations normal to the direction of growth, the hardness numbers are 183 and 179 from top to bottom in Figure 7b. Since the hardness numbers in a given direction are relatively close, the average hardness number may be considered as 213 and 181 for the direction parallel and normal to the growth of the grains, respectively. The hardness numbers differs by approximately 15 percent between the two directions.

One reason for the difference in hardness between the directions parallel and normal to the direction of crystal growth is the columnar type of crystal structure which is present. Because of the small grain size normal to the crystal growth direction, there are numerous grain boundaries, some of which were encountered during the hardness test, thus increasing the hardness obtained.

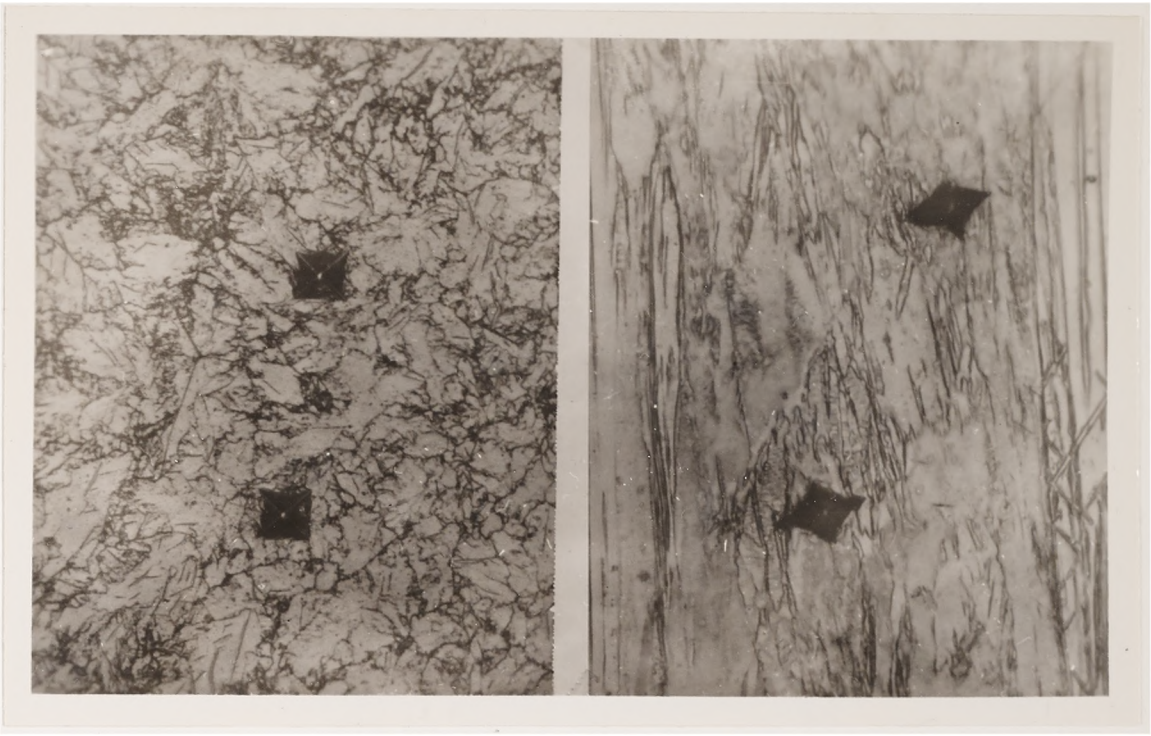

a b

Figure 7. Microhardness Impressions in Electrodeposited Cobalt: (a) Section Normal to Crystal Growth; (b) Section Parallel to Crystal Growth. 325X.

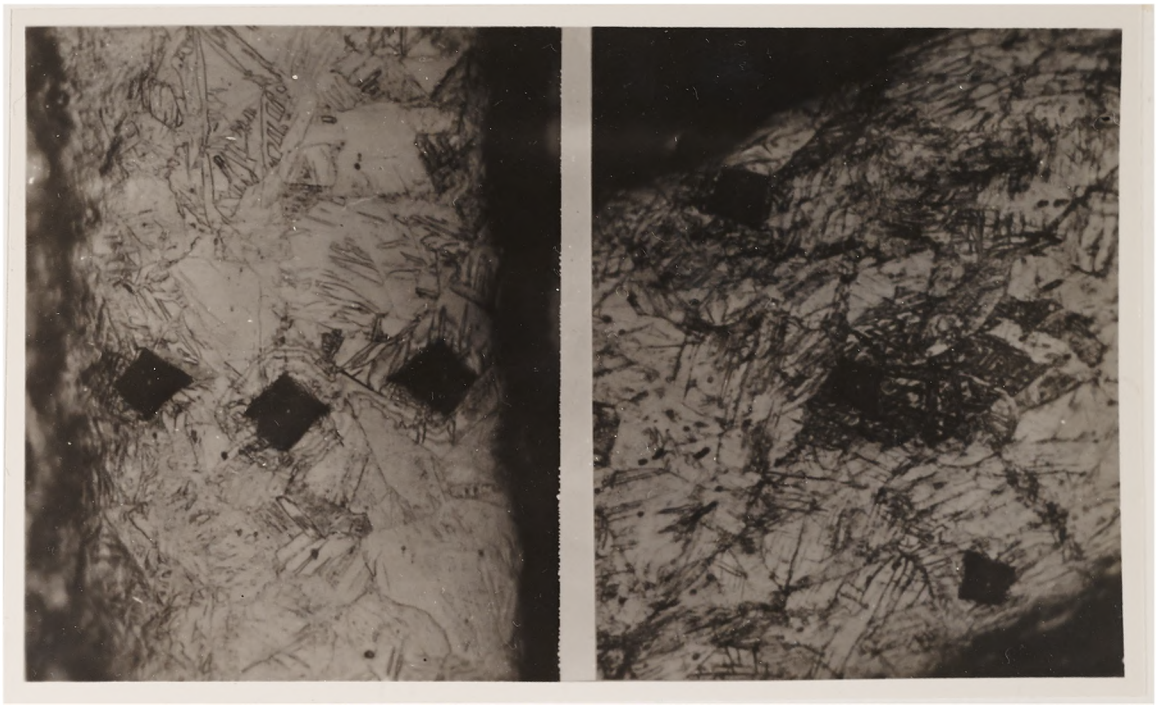

a b

Figure 8. Microhardness Impressions in Cold Rolled Sintered Cobalt Powder: (a) 5 Percent Reduction; (b) 15 Percent Reduction. Both Sections Are Parallel to Rolling Direction. 325X.

Rolled Cobalt Powder. Figure 8 shows the results of the microhardness test in five percent and fifteen percent rolled cobalt powder. In both samples the hardness tests were made normal to the rolling direction and also normal to one edge of the samples.

In the specimen reduced five percent by cold rolling (Figure 8a), the DPH numbers for the indentations from left to right in the photomicrograph are 156, 154 and 146. An inspection of the five percent rolled powder shows concentric deformation lines around each indentation, resulting from the deformation during the penetration of the diamond indentor. As can be seen, these deformation lines for the central and far right indentations intersect. Because the central indentation was the last one of the series to be made, the deformation from the indentation at the right probably caused the abnormal increase in hardness of the former indentation.

In the specimen reduced fifteen percent by cold rolling (Figure 8b), the DPH numbers for the indentations from bottom to top in the photomicrograph are 264, 242 and 222. The twinned area in which the central indentation was made accounts for the increase in this area. The reason for the very high hardness at the bottom of the photomicrograph is that the center of the indentation is closer to the edge of the specimen than the impression at the top. This sample was difficult to etch, and consequently the area chosen for the indentation may be twinned parallel to the surface and not normal to the

surface as in the area of the central indentation.

Even with the wide difference in hardness numbers, there is proof that hardness at the surface is greater than that at the center of a rolled sample. With a comparison of the two rolled samples, it is evident that the microhardness increases with the amount of cold deformation.

Cold Rolled Annealed Sponge. Figure 9 shows the hardness indentations in the annealed specimen and specimens reduced ten and forty percent by cold rolling. For the sample without cold work, (Figure 9a) the DPH in the twinned area is 215 while that in the untwinned area is 194. The hardness of this latter area is affected by the neighboring twinned areas which increase the hardness. This hardness increase due to neighboring twinned areas is illustrated by Figure 15a showing an indentation in a large untwinned region. The hardness of this latter area is 179 which is eight percent lower than the other untwinned region in Figure 9a. The twins in this sample are a result of the allotropic transformation from face-centered cubic to hexagonal close-packed structure when cooling from the annealing temperature of 1176°C.

For the ten percent cold-rolled annealed sponge (Figure 9b), there is a general increase in hardness over that of the sponge without deformation. The DPH of the untwinned region is now 202 while that of the twinned region is now 287. The

effect of the boundary between the untwinned and twinned regions is shown by the third indentation on the boundary. The hardness at this point is 268 which is between the hardness of the two regions. Thus, these hardness values show that the twinned area has more effect on the hardness at a boundary than the untwinned region, since the boundary hardness approaches that of the twinned region.

In the forty percent cold-rolled annealed sponge (Figure 9c), the DPH has increased to approximately 280, which is an increase over the ten percent rolled sample. The DPH of the three indentations shown in the photomicrograph from top to bottom are 283, 264, 281. Because forty percent reduction was the maximum obtainable without complete failure of the sample, the sample should be almost completely twinned. The amount of twinning in Figure 9c is relatively small but increases toward the opposite side of the sample, where the hardness increases progressively to 508 at the other edge. The impressions across the sample are shown in Figure 10. The impressions at the top of Figure 10 correspond to those in Figure 9c. The effect of a heavily twinned region in this sample is shown in Figure 11, where the DPH is 417.

Hardness readings were made at the end and to the left of the crack shown in the lower left corner of Figure 10. The three hardness impressions around the end of the crack are shown in Figure 12. The DPH numbers for these impressions are 272 at the top right, 299 at the end of the crack, and 306 at

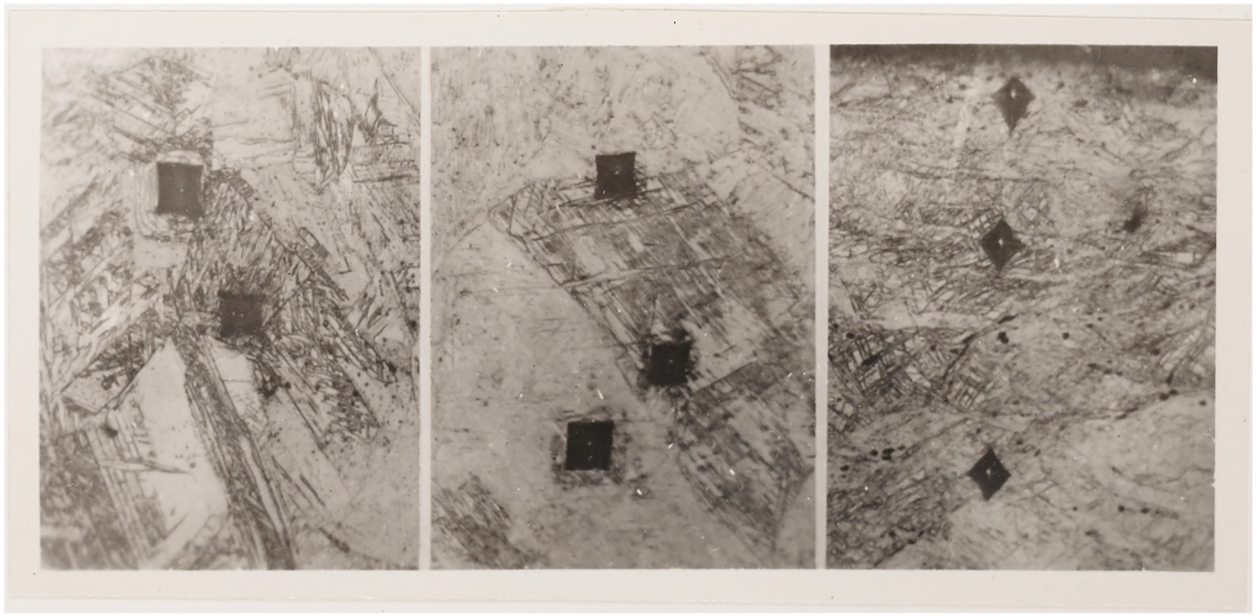

a b c

Figure 9. Microhardness Impressions in Annealed Cobalt Sponge: (a) Annealed; (b) Cold Rolled 10 Percent; (c) Cold Rolled 40 Percent. All Impressions Were Made Normal to Rolling Plane. 275X.

Figure 10. Microhardness Impressions in 40 Percent Cold Rolled Annealed Cobalt Sponge. 100X.

Figure 11. Microhardness Impressions in a Twinned Area in a 40 Percent Cold Rolled Annealed Cobalt Sponge. 350X.

Figure 12. Microhardness Impressions Around the End of a Crack in the 40 Percent Cold Rolled Annealed Sponge. 650X.

the lower right. There is approximately eleven percent difference in the hardness numbers. The DPH along the crack increases to 370 toward the opposite end of the crack and then decreases to 342 at the intersection of the crack with the surface. Since the hardness should be greater at the ends of a crack than at the center due to the increased number of dislocations at the ends of a crack, the hardness number of 370 must have been the result of a highly stressed region which could not be seen under the microscope. The high hardness at the edge corresponds to the high hardness at the same edge in Figure 10.

Effect of Crystal Orientation. Additional hardness readings were made on the annealed sponge without cold reduction to illustrate the effect of grain orientation on the hardness. An annealed sponge sample was chosen because of the characteristically large grain size in this material.

Figure 13 shows the results of the grain orientation effects. Figure 13b was made using polarized light to illustrate the difference in grain orientation. There is a wide difference of hardness as a result of the difference in orientation of the grains. The hardness of the large grain in the center of the photomicrograph is 206 while the hardness of the other light-colored grain is 187. Under bright-field illumination, the orientation of these two grains might be the same. However, under polarized light, the difference in

orientation of the grains is obvious.

The hardness in the region of the third impression, which appears to be a twinned area, is 214 DPH. The orientation in this grain is again different from the other two grains. Because the hardness of the large light-colored grain closely approaches that of the twinned grain, the former grain must have some twinning in which the orientation is such that the twinning is not evident with microscopic examination. This twinning may be proven to exist by what appears to be some visible twinning in the left half of the large light-colored grain.

Deformation Lines. During the microhardness test, deformation lines were noticed which were concentric around the hardness impressions. Again, the annealed sponge without cold rolling was used to study these "lines". Figures 14 and 15 show the deformation lines about the hardness impression in the annealed sponge. Figure 14 is the same area as Figure 9a.

From the examination of these Figures, deformation lines are seen to be concentric about the indentations. The deformation lines cross grain boundaries but are not as pronounced in twinned regions as in the untwinned regions (Figure 14). Thus, more deformation is caused in the relatively undistorted grains than in the distorted grains.

In comparing the deformation lines in Figure 15a

a b

Figure 13. Microhardness Impressions in Annealed Cobalt Sponge Showing the Effect of Grain Orientation: (a) Bright-Field Illumination; (b) Polarized Light. 300X.

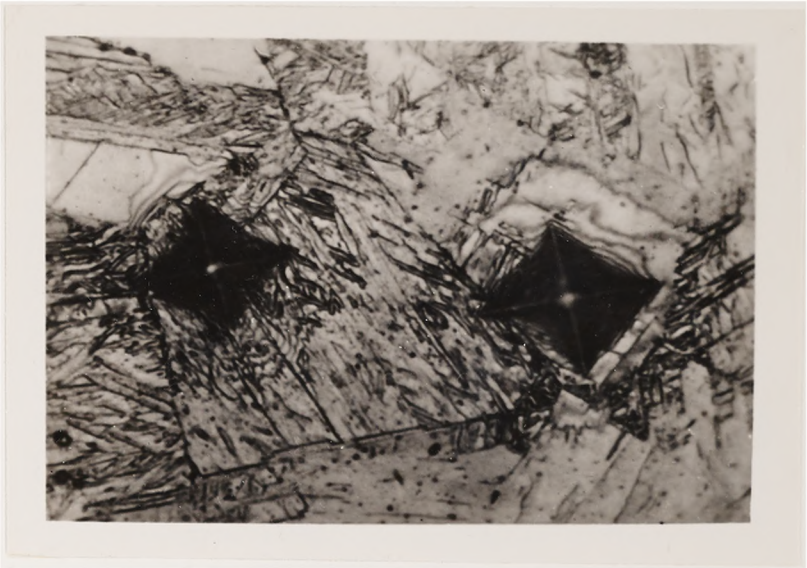

Figure 14. Deformation Lines as a Result of Microhardness Impressions in Annealed Cobalt Sponge. 650X.

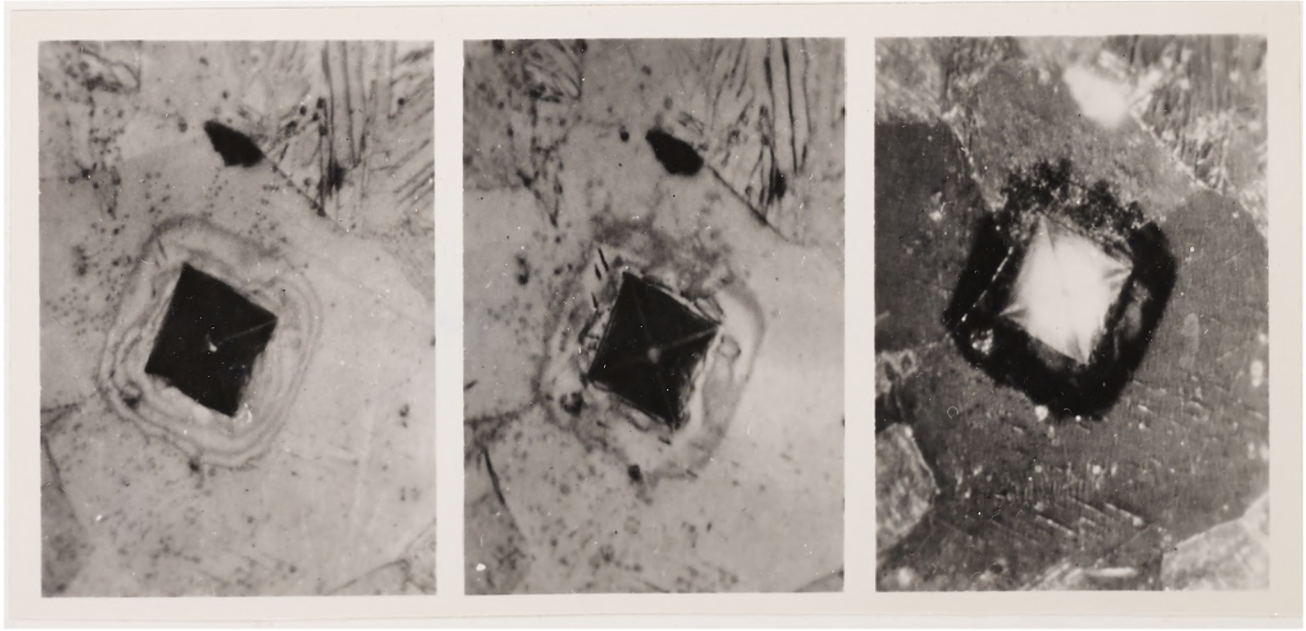

a b c

Figure 15. Deformation Lines as a Result of Microhardness Impressions in Annealed Sponge: (a) Immediately After Deformation; (b) 12 Hours After Deformation; (c) 12 Hours After Deformation Under Polarized Light. 550X.

immediately after the hardness test and again twelve hours after the test in Figure 15b, it is seen that the deformation lines have become fewer and broader with time. This decrease in the number of the deformation lines and their broadening indicates that the material has flowed to relieve the stress caused by the penetration of the indentor.

To prove that these lines are caused by deformation and are not the result of discoloration or light interference, the impression was photographed using polarized light. Figure 15c shows the results of polarized light, and as seen by the black regions around the impression, this area is a result of deformation. Also, in this photomicrograph, the effect of grain orientations on the deformation lines can be observed.

Summary. The following results were obtained by performing microhardness tests on various cobalt structures:

1. Microhardness in electrodeposited cobalt is greater parallel to the direction of crystal growth than normal to the direction of growth.

2. The overall hardness increased with the amount of cold rolling for both rolled powders and annealed sponge.

3. Microhardness was found to be dependent upon crystal orientation of individual grains.

4. Less deformation resulted from the penetration of the diamond indentor in the twinned regions than in the untwinned regions, with the twinned regions having a higher

microhardness.

5. The penetration of the indentor caused deformation lines which were concentric around the impression. These lines broadened and decreased in number with time, indicating that some plastic flow of the deformed material occurred at room temperature.

CHAPTER V

X-RAY EXAMINATION

A. PREPARATION OF X-RAY SAMPLES

With the use of the universal specimen mount constructed by Williams, (30) (31) a refinement of the Decker and Schulz X-ray technique, two specimens are required, one for transmission intensities and one for reflection intensities. To prevent the specimen from forming a surface texture as a result of polishing, the specimen preparation for X-ray examination was made by etching only.

Preparation for Transmission. If the thickness of the samples is controlled, no correction for absorption is necessary with transmission methods. However, the necessary thickness required to eliminate the absorption correction is so small that it was impossible to obtain by the techniques used. Therefore, the thickness of the samples had to be determined to correct for absorption. The Decker (32) method

---

(30) D.N. Williams, "An Investigation of the Deformation Texture of Titanium", University of Missouri, Ph.D. Dissertation, (M.S.M. - T1036), 1952.

(31) D.N. Williams and D.S. Eppelsheimer, "Universal Speciman Mount for Pole Figure Determination Using the Schulz-Decker Techniques", Missouri School of Mines Technical Bulletin, No. 79, January, 1952.

(32) B.F. Decker, E.T. Asp, and D. Hacker, "Preferred Orientation Determinations Using a Geiger Counter X-Ray Diffraction Goniometer", Journal of Applied Physics, Vol. 19, p. 388, 1948.

was used for the determination of the thickness of transmission samples.

The value of the (110) alpha brass reflection was measured with the counter opened. Then the counter was covered with the cobalt transmission sample, and the intensity of the brass reflection measured again. These intensities are I_o and I_t, respectively, and are used to calculate μt, where μ is the absorption coefficient of cobalt. This calculation was performed using the absorption equation (33)

$$\mu t = \ln I_o/I_t. \qquad (5)$$

The value of μt was then substituted into the absorption correction formula to determine the necessary corrections.

The transmission samples were prepared by etching on one side only. This was done by coating one side of the sample with paraffin and exposing the other side to the etching solution.

Preparation for Reflection. The reflection technique is based on the assumption that the reflection sample is thick enough for the incident beam to be completely absorbed in the sample. (34) Therefore, to determine the minimum

---

(33) B.D. Cullity, Elements of X-Ray Diffraction, (Reading, Mass.: Addison-Wesley, 1956), p. 10.

(34) L.G. Schulz, "A Direct Method of Determining Preferred Orientation in Flat Reflection Samples Using a Geiger Counter X-Ray Spectrometer", Journal of Applied Physics, Vol. 20, pp. 1030, 1949.

thickness required, a ratio of I_o to I_t of 1000 to 1 was assumed for total absorption. The value of the minimum thickness was found to be 0.0037 inches, when μ is 727 per centimeter for cobalt using iron radiation. This value was calculated using the absorption equation.

$$\begin{aligned} \mu t &= \ln I_o/I_t \\ &= \ln 1000/1 \\ \mu t &= 6.9078 \\ t &= .0037 \text{ inches} \end{aligned} \qquad (5)$$

Because this minimum value of thickness is rather small, control of sample thickness was not required. However, all reflection samples were at least 0.02 inches in thickness. The reflection samples were prepared by etching a few mils below the surface to eliminate possible surface effects.

Etching Techniques. The etching solution used was a mixture of hydrofluoric acid, nitric acid, and water. A ratio of 1:3:5 by volume gave a more uniform etch than the other ratios tested. Also, the heat of reaction between the cobalt and this ratio of reactants was not high enough to melt the protective paraffin coating when etching only on one side of the specimen was required.

B. X-RAY TECHNIQUE

Pole figures were constructed using the Schulz-Decker Geiger counter technique with the aid of a universal specimen mount. This specimen mount is discussed thoroughly by Williams. (35) (36) This mount does not allow movement of the samples in an oscillatory manner to permit scanning of the specimens. Intensities of the $10\bar{1}0$, 0002, and $10\bar{1}1$ lines were measured and after absorption and defocusing corrections, the pole figures were drawn.

Measurement of Intensities. Intensities of the diffracted X-rays from the $(10\bar{1}0)$, (0002), and $(10\bar{1}1)$ planes of the sheet materials were measured at every ten-degree interval of latitude and longitude for one quadrant of a polar stereographic net for the determination of the pole figures. Transmission intensity readings were made from 0° to -30° latitude. Reflection intensity readings were from -30° to -90°. The region of overlapping at -30° was used as a means of correlating the transmission and reflection data. All X-ray examinations of sheet material were made using filtered iron radiation.

Plotting of Pole Figures. The corrected intensity

---

(35) Williams, Loc. cit.

(36) Williams and Eppelsheimer, Loc. cit.

data were plotted directly on a polar stereographic net. This could be done since the intensity measured by the X-ray spectrometer is directly proportional to the density of the pole figure.

CHAPTER VI

THE COLD-ROLLED TEXTURES OF COBALT

A. EXPERIMENTAL RESULTS

Three types of high-purity cobalt were used to determine the cold-rolled textures of cobalt. These types were rolled electrodeposited cobalt, rolled cobalt powder, and rolled annealed sponge. The texture of the cold-rolled electrodeposited cobalt was found to be different from the rolling textures of cobalt obtained from other sources. This difference in texture was the result of the partial retention of the electrodeposited texture after annealing.

Textures of Cold-Rolled Electrodeposited Cobalt. Four different samples were used to determine the cold-rolled texture of electrodeposited cobalt. These samples consisted of the "as-received" deposited cobalt, the "as-received" cobalt cold-rolled eight percent, the "as-received" cobalt after annealing for 100 hours at 840°F, and the "as-received" material in the annealed condition cold-rolled twenty percent.

The texture of the "as-received" electrodeposited cobalt is discussed to illustrate the effects of this texture in the rolled and annealed materials. The $(10\bar{1}1)$, (0001), and the $(10\bar{1}0)$ pole figures are given in Figure 16. The (0001) pole figure shows a maximum at the $[10\bar{1}0]$ position

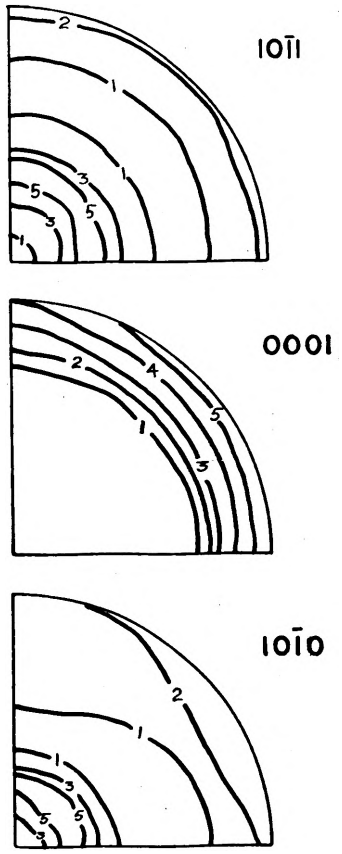

FIGURE 16. THE $(10\bar{1}1)$,(0001), AND $(10\bar{1}0)$ POLE FIGURES FOR ELECTRODEPOSITED COBALT.

with a spread through the $[11\bar{2}0]$ to the $[01\bar{1}0]$ position. In both the $(10\bar{1}0)$ and the $(10\bar{1}1)$ poles the maximum is rotated thirty degrees radially about the center of the pole signifying random orientation.

Therefore, the texture of the electrodeposited cobalt is mainly $[10\bar{1}0]$ with a large spread in the texture toward the $[11\bar{2}0]$ direction. This means that the hexagonal axis is normal to or the (0001) plane is parallel to the direction of crystal growth, since the $[10\bar{1}0]$ and the $[11\bar{2}0]$ directions lie in the (0001) plane and are parallel to the direction of growth. The orientations of the (0001) planes, the hexagonal axis, and all other planes are such as to be completely random about the direction of crystal growth.

This mixed texture is not in complete agreement with Wassermann, (37) who reported the texture of deposited films of cobalt to be the $[110]$ direction. However, in the reported work, the cobalt was deposited from a sulfate solution on a copper electrode in the form of a thin film, in which case the film may have had a texture which was influenced by the base metal. In the present investigation, the cobalt was not a thin film but was between 0.05 and 0.08 inches in thickness. The texture of a deposit of this thickness should no longer be influenced by the base metal because this

---

(37) B. Wassermann, Texture of Metallic Materials, (Berlin: Julius Springer, 1939), p. 310.

influence does not extend very far into the deposited metal (38) and thus the deposited metal is free to develop its own texture.

The total amount of cold reduction, without an initial heat treatment, that could be given to the electrodeposited cobalt without cracking was approximately eight percent. As shown in Figure 1, by the time cold reduction had reached eleven percent, the sample had broken into seven pieces. The rolling direction is always normal to the direction of crystal growth in these electrodeposited samples. Because of the gradual reorientation of the lattice during plastic deformation, little preferred orientation is produced below twenty to thirty percent reduction, and thus, little change in the texture is expected with eight percent reduction. This unchanged texture from the undeformed electrodeposited cobalt is confirmed by the examination of the pole figures for the deformed cobalt.

The $(10\bar{1}1)$, (0001) and the $(10\bar{1}0)$ pole figures for the eight percent cold-rolled electrodeposited cobalt are shown in Figure 17. In comparison with Figure 16 for the "as-received" cobalt, the $(10\bar{1}0)$ and the $(10\bar{1}1)$ poles show very little change with only a decrease in the spread of the maximum in each case with increased cold rolling. Thus,

---

(38) C.L. Barrett, Structure of Metals, (New York: McGraw-Hill, 1954), p. 514.

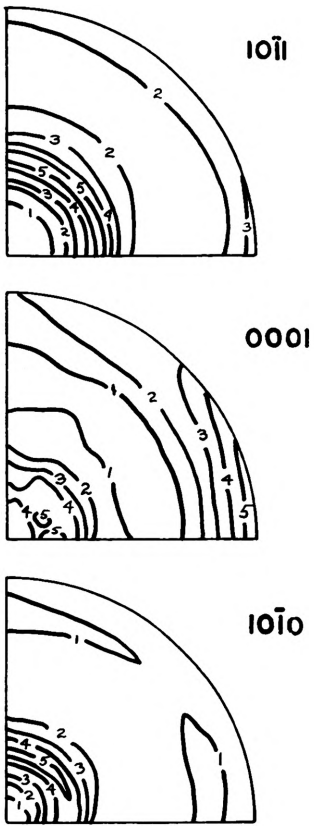

FIGURE 17. THE (10$\bar{1}$1), (0001), AND (10$\bar{1}$0) POLE FIGURES FOR ELECTRODEPOSITED COBALT REDUCED 8 PERCENT BY COLD ROLLING.

the random orientation about the direction of crystal growth has not changed.

The only noticeable change in the pole figures for the eight percent cold-rolled cobalt occurs in the (0001) pole. Superimposed on the texture of the undeformed sample is a texture due to deformation. A maximum still exists in the lower right portion of the pole, which is now the transverse direction. This maximum in the $[10\bar{1}0]$ direction has decreased in area in the rolled condition and has moved into the $[10\bar{1}0]$ direction with very little spread toward the $[\bar{1}2\bar{1}0]$ direction. Also with deformation, the intensity in the central portion of the pole has increased up to tenfold over that in the undeformed condition. Due to the deformation, another maximum occurs which is rotated twenty degrees from the rolling plane normal in the transverse direction. Thus, it is seen with rolling of electrodeposited cobalt, the maximum shifts toward the rolling plane normal by superimposing the deformation texture on the undeformed texture for the (0001) pole.

Because the rolling direction in the electrodeposited cobalt samples was normal to the direction of crystal growth, it is reasonable to assume that in rolling, for this case, the compression effects of rolling would overshadow the tension effects. Because slip rotations in the three possible slip systems in hexagonal crystals, the $(0001)\langle 11\bar{2}0\rangle$, $(10\bar{1}1)\langle 11\bar{2}0\rangle$, and the $(10\bar{1}0)\langle 11\bar{2}0\rangle$ systems, and $\{10\bar{1}2\}$

twinning do not lead to a concentration of the (0001) poles toward the rolling plane normal in tension, compression must be the main method of deformation. In order to account for the observed shifting of the (0001) pole during deformation of electrodeposited cobalt, the mechanism of deformation is by (0001) $\langle 11\bar{2}0 \rangle$ slip and $\{10\bar{1}2\}$ twinning in compression, because the rotations involved with these mechanisms lead to a concentration of the (0001) poles at the rolling plane normal. Rotations involved with $(10\bar{1}1)\langle 11\bar{2}0\rangle$ and $(10\bar{1}0)\langle 11\bar{2}0\rangle$ slip in compression move the (0001) pole away from the rolling plane normal in the $[11\bar{2}0]$ direction.

In order to increase the amount of cold rolling of the electrodeposited cobalt without failure, the deposited material was given an annealing treatment at 840°F for 100 hours. The effects of this heat treatment on the "as-received" deposited cobalt are discussed here for a comparison with cold-rolled deposited cobalt after this heat treatment.

The $(10\bar{1}1)$, (0001) and the $(10\bar{1}0)$ pole figures for the annealed electrodeposited cobalt are shown in Figure 18. As it may be seen from these pole figures, there is very little preferred orientation. The annealing temperature of 840°F was approximately 50°F above the allotropic transformation of the hexagonal close-packed structure to the face-centered cubic structure. Some of the high-temperature structure (f.c.c.) was retained in the sample after

annealing, and the (200) pole figure for the cubic phase is shown in Figure 19. The retention of the cubic phase resulted in the overlapping of the hexagonal (0002) diffraction lines and the cubic (111) diffraction lines, which could not be resolved due to the very small difference in the Bragg angles of diffraction when using iron radiation. The (111) planes in the face-centered cubic system are the transformation planes for the allotropic transformation and transform into the (0002) planes in the hexagonal close-packed system. (39) The difficulty of not resolving these two diffraction lines was solved to some extent by weighting the (0002) lines twice that of the (111) lines when correcting for defocusing. As a result the (0001) pole is a combination of the (0001) and the (111) intensities and not too much significance can be applied to this pole figure. About the only relationships that can be derived from these poles is that there is a tendency for the intensities to be ninety degrees from the central portion of the pole figures. Because of the small amount of preferred orientation a three-fold increase in the maximum allowable cold reduction was obtained after annealing above the allotropic transformation temperature.

The annealing treatment of the electrodeposited

---

(39) H. Bibring, F. Sebilleau, and C. Buckle, "The Kinetics and Morphology of the Allotropic Transformation of Cobalt", Journal of Metals, Vol. 87, pp. 71-73, 1958.

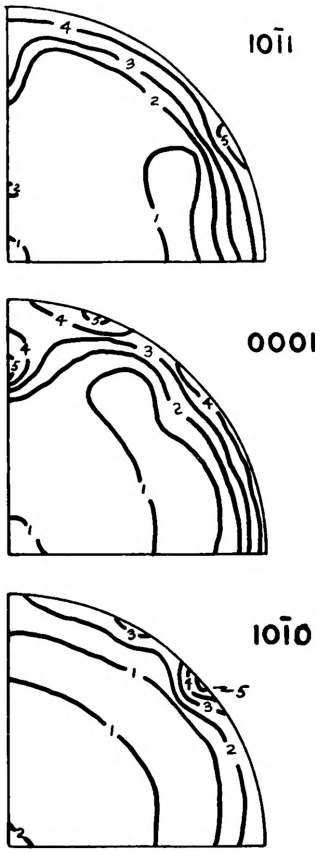

FIGURE 18. THE (10$\bar{1}$1), (0001), AND (10$\bar{1}$0) POLE FIGURES FOR ELECTRODEPOSITED COBALT ANNEALED 100 HOURS AT 840°F.

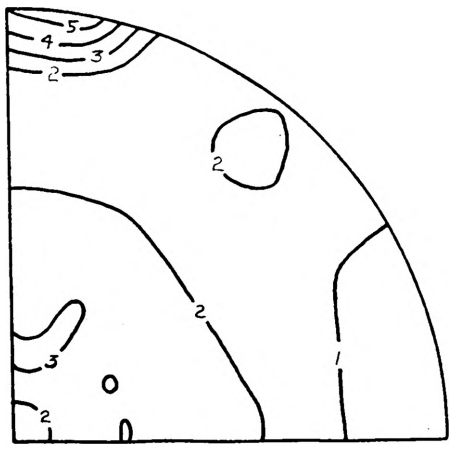

FIGURE 19. THE (200) POLE FIGURE FOR THE RETAINED FACE-CENTERED CUBIC PHASE IN ELECTRODEPOSITED COBALT ANNEALED FOR 100 HOURS AT 840°F.

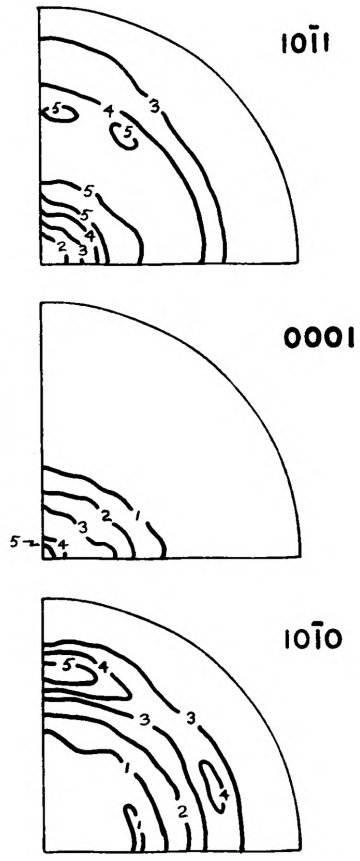

FIGURE 20. THE (10$\bar{1}$1), (0001), AND (10$\bar{1}$0) POLE FIGURES FOR ELECTRODEPOSITED COBALT REDUCED 20 PERCENT BY COLD ROLLING AFTER ANNEALLING 100 HOURS AT 840°F

cobalt increased the allowable cold rolling without failure to twenty percent. Even with this amount of deformation a representative texture of cobalt is not produced, because the reduction is not great enough. Therefore, the texture of twenty percent cold-rolled electrodeposited cobalt with an initial heat treatment can be described as a mixture of $(0001)\langle 11\bar{2}0\rangle$ texture and $[10\bar{1}0]$ fiber axis. This mixed texture results from the deformation texture of the type $(0001)\langle 11\bar{2}0\rangle$ and the partial retention of the deposited fiber axis of $[10\bar{1}0]$.

The $(10\bar{1}1)$, (0001) and the $(10\bar{1}0)$ pole figures for the twenty percent cold-rolled deposited cobalt after annealing is shown in Figure 20. The (0001) pole shows a maximum at the rolling plane normal which is usually the position of highest intensity in hexagonal close-packed metals with c/a ratio less than 1.633.

The $(10\bar{1}0)$ pole shows a maximum rotated twenty degrees in the rolling direction from the $[0001]$ position toward the $[10\bar{1}0]$ and spreading toward the $[11\bar{2}0]$. This spread indicates an incomplete rotation of the $[11\bar{2}0]$ into the rolling direction.

The $(10\bar{1}1)$ pole shows little preferred orientation. In this case, the largest maximum is rotated radially thirty-five degrees about the center of the pole. However, there is a secondary maximum at the $[000\bar{1}]$ position.

Thus, the amount of deformation given to the annealed electrodeposited cobalt was not great enough to completely destroy the retained texture of the deposited cobalt after annealing above the transformation temperature. The annealing treatment does not completely remove the orientation of the original hexagonal crystals because the original hexagonal crystals have a high probability of being recovered after the heat treatment. (40) Therefore, the texture of cold-rolled deposited cobalt after annealing can be described as a (0001) $\langle 11\bar{2}0 \rangle$ texture in which some of the original $[10\bar{1}0]$ fiber axis is retained.

Texture of Cold-Rolled Cobalt Powder. The $(10\bar{1}1)$, (0001) and the $(10\bar{1}0)$ pole figures of cobalt powder strip reduced fifteen percent are shown in Figure 21. The texture can be described as a (0001) $\langle \bar{1}2\bar{1}0 \rangle$ texture in which the (0001) plane is rotated twenty-five degrees in the rolling direction with the $\langle \bar{1}2\bar{1}0 \rangle$ rotated twenty-five degrees in the transverse direction. Even though the maximum rolling was fifteen percent, the texture is fairly well developed due to the small thickness of the strip (order of 0.01 inches in thickness) and the previous history.

The (0001) pole in Figure 21 shows a maximum about twenty-five degrees from the rolling plane normal in the

---

(40) Bibring, Sebilleau, and Buckle, Loc. cit.

rolling direction with a slight spread of the lowest intensity contour towards the transverse direction. This spread of the low-intensity contours towards the transverse direction may also be seen in the (0001) poles for the five and ten percent reduced cobalt powder strip shown in Figure 22. Also, in the comparison of the three (0001) poles for five, ten, and fifteen percent reduction, it is seen that the areas of the maxima and the spread of the maxima toward the transverse direction decrease as the percent reduction increases. Thus, as deformation increases for these low reductions, there is a tendency for the (0001) pole to rotate twenty-five degrees from the rolling plane normal toward the rolling direction, giving a (0001) $\langle\bar{1}2\bar{1}0\rangle$ texture. However, due to the spread of the low intensities toward the transverse direction and the spread of the maximum in the five percent sample in this same direction, there is also a small tendency for the (0001) $\langle 10\bar{1}0\rangle$ texture. This latter texture, however, seems to become less important as reduction increases. The fairly high intensity at the rolling plane normal should be noted, since this position is that which usually has highest intensity in hexagonal close-packed metals with c/a ratio less than 1.633.

In the $(10\bar{1}0)$ pole for the fifteen percent reduced cobalt powder strip, the position of the primary maximum corresponds to a rotation of twenty-five degrees from the

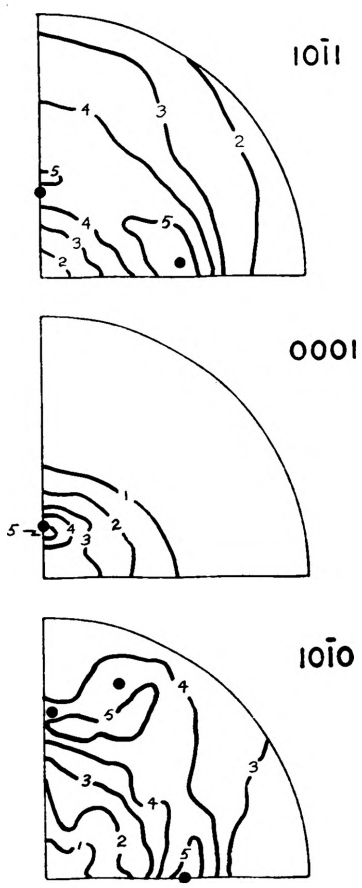

FIGURE 21. THE (10$\bar{1}$1),(0001), AND (10$\bar{1}$0) POLE FIGURES FOR 15 PERCENT COLD-ROLLED SINTERED COBALT POWDER STRIP.

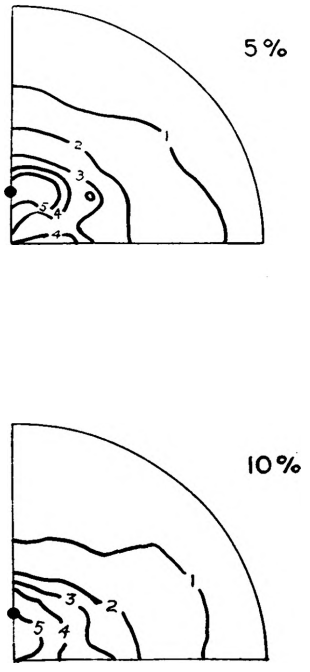

FIGURE 22. THE (0001) POLE FIGURES FOR 5 AND 10 PERCENT COLD-ROLLED SINTERED COBALT POWDER STRIP. ● ---(0001)[$\bar{1}2\bar{1}0$] ROTATED 25 DEGREES IN ROLLING DIRECTION.

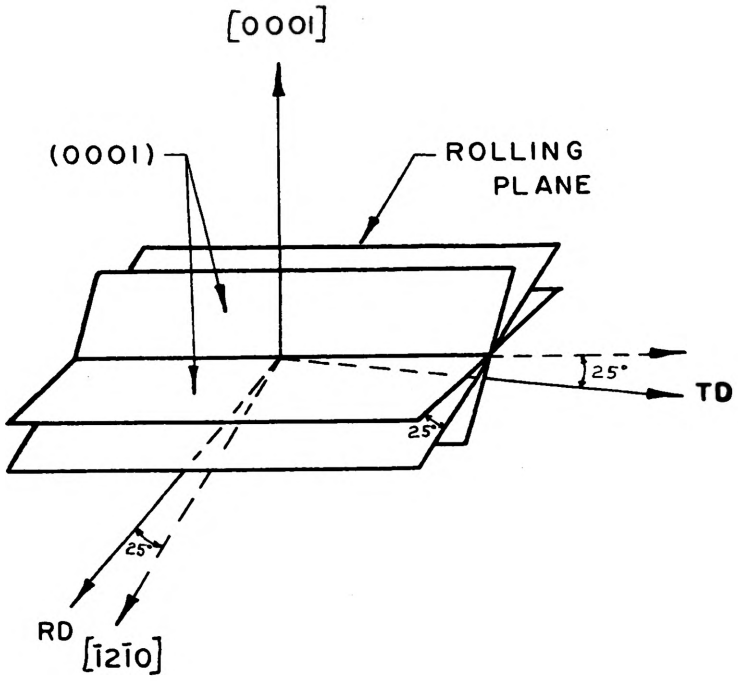

FIGURE 23. SCHEMATIC REPRESENTATION OF THE DEFORMATION TEXTURE OF COLD-ROLLED COBALT POWDER STRIP.

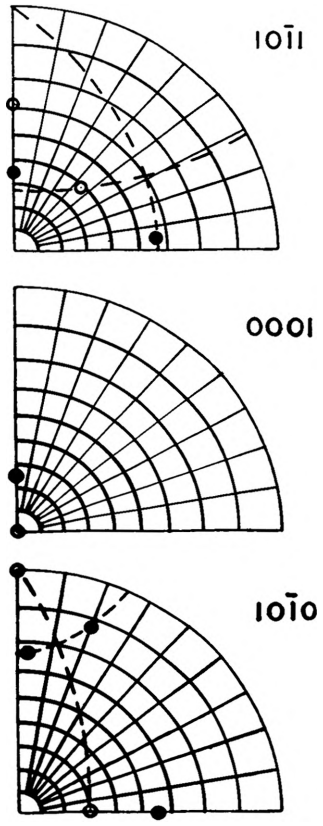

FIGURE 24. POSITION OF IDEAL TEXTURE: O -- $(0001)[\bar{1}2\bar{1}0]$; ● -- $(0001)[\bar{1}2\bar{1}0]$ ROTATED 25° IN BOTH ROLLING AND TRANSVERSE DIRECTIONS.

rolling direction toward the $[11\bar{2}0]$ position with a spread of twenty-five degrees both right and left in the transverse direction. The second maximum is located by a twenty-five degree rotation in the transverse direction about the $[11\bar{2}0]$ position. The intensity in the rolling direction is approximately four times that at the $[10\bar{1}0]$ position which is the minimum and approximately twice that at the $[\bar{1}2\bar{1}0]$ position. The maxima in the $(10\bar{1}1)$ pole correspond to a rotation of twenty-five degrees in the rolling direction from the $[000\bar{1}]$ position and a double rotation of twenty-five degrees in both the rolling and transverse directions about the $[11\bar{2}0]$ position.

The pole figures of the cold-rolled cobalt powder strip are influenced by two main factors. The first is the tendency of the $[\bar{1}2\bar{1}0]$ direction to be rotated twenty-five degrees from the rolling direction, and the second is the tendency for the (0001) pole to be rotated twenty-five degrees from the rolling plane normal toward the rolling direction. These conditions can be the result of (0001) $\langle\bar{1}2\bar{1}0\rangle$ slip accompanied by mechanical twinning, such as $\{10\bar{1}2\}$. Pictorially, the observed texture for rolled cobalt powder strip is shown in Figure 23. Figure 24 shows the necessary rotations for the observed textures plotted over a polar stereographic net. The white circles are before rotation and the black circles are after rotation.

Since rolling consists of compression normal to the rolling plane and tension parallel to the rolling direction, rolling textures are therefore a combination of tension and compression textures.

With the use of a resolved shear stress contour diagram plotted in the hexagonal stereographic triangle consisting of $[0001]$ - $[\bar{1}2\bar{1}0]$ - $[10\bar{1}0]$ edges, the (0001) $\langle 11\bar{2}0\rangle$ slip system in tension causes a rotation to a $\langle 11\bar{2}0\rangle$ texture with a spread of orientations along the $[11\bar{2}0]$ - $[10\bar{1}0]$ edge. Compression rotations for this system lead to a strong $[0001]$ texture. With the addition of $\{10\bar{1}2\}$ twinning, these relationships are reinforced. The $\{10\bar{1}2\}$ twinning assists slip rotations by twinning toward the $[0001]$ in compression and toward the $[10\bar{1}0]$ - $[11\bar{2}0]$ edge of the unit triangle in tension.

Texture of Cold-Rolled Cobalt Sponge. The $(10\bar{1}1)$, (0001) and the $(10\bar{1}0)$ pole figures of rolled cobalt sponge reduced forty percent are shown in Figure 25. The texture can be described as a (0001) $\langle \bar{1}2\bar{1}0\rangle$ texture in which the (0001) plane is rotated twenty to twenty-five degrees in the rolling direction with the $\langle \bar{1}2\bar{1}0\rangle$ rotated twenty to twenty-five degrees in the transverse direction.

The (0001) pole in Figure 25 shows a maximum about twenty degrees from the rolling plane normal in the rolling direction. The tendency for this rotation can be seen in the (0001) poles for ten, twenty, and thirty percent reduced

sponge in Figure 26. In comparing these four poles, it is seen that the maximum is rotating away from the rolling plane normal in the rolling direction. Unlike the case for the rolled powders, the maxima in the (0001) poles do not spread much toward the transverse direction in the low reduction samples. However, like the rolled powder samples, there is still a rather high intensity at the rolling plane normal indicating that the same mechanisms operating in the rolled powder still operate in the rolled sponge.

In the $(10\bar{1}0)$ pole for the forty percent rolled sponge, the position of the maximum corresponds to a rotation of thirty degrees in the rolling direction toward $[11\bar{2}0]$ with a rotation of thirty degrees in the transverse direction. In the $(10\bar{1}0)$ poles of the ten, and thirty percent rolled sponge which are not shown, the maximum decreases from a large spread in the transverse direction across the pole to the rolling direction, being rotated thirty degrees from the rolling direction in the twenty percent sample to a smaller maximum in the thirty percent sample which is rotated thirty degrees in the rolling direction toward the $[11\bar{2}0]$ with a rotation of forty degrees in the transverse direction. Thus, the position of the maximum in the $(10\bar{1}0)$ pole is moving toward a thirty degree rotation from the rolling direction toward the $[11\bar{2}0]$. However, in order to correlate the experimental results, the rotation occurring with forty percent reduction must be a double

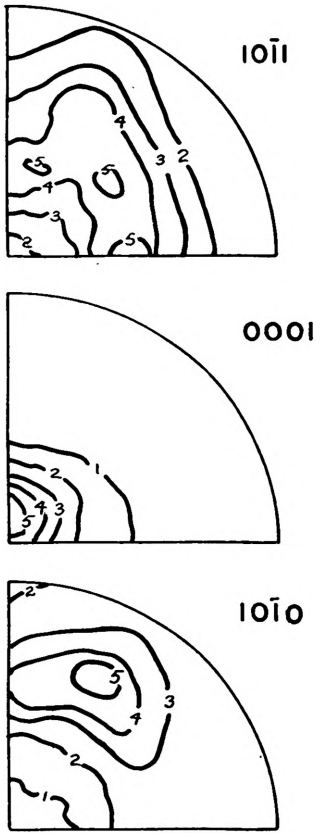

FIGURE 25. THE (10$\bar{1}$1), (0001), AND (10$\bar{1}$0) POLE FIGURES FOR ANNEALED SPONGE REDUCED 40 PERCENT BY COLD ROLLING.

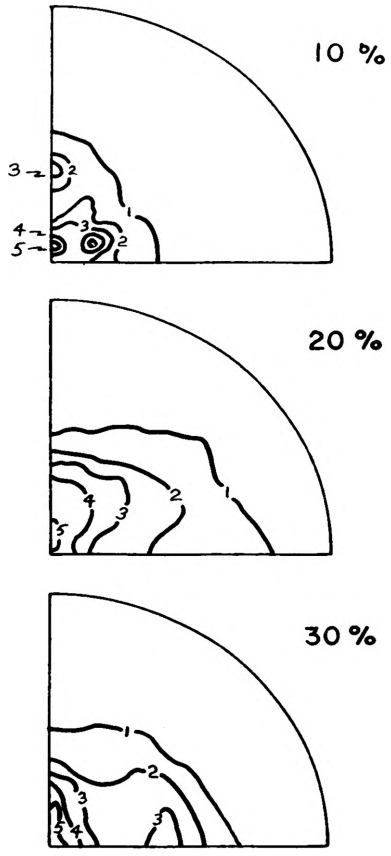

FIGURE 26. THE (0001) POLE FIGURES FOR ANNEALED SPONGE REDUCED 10, 20, AND 30 PERCENT BY COLD ROLLING.

rotation of twenty to twenty-five degrees in both the rolling and transverse directions. The higher intensity in the rolling direction over that in the transverse direction should be noted.

The $(10\bar{1}1)$ pole shows three maxima, one of which is rotated twenty-five degrees from the $[000\bar{1}]$ in the rolling direction and twenty-five degrees in the transverse direction. The other maxima can be described as: (1) a twenty-five degree rotation in the transverse direction from the $[11\bar{2}0]$ and, (2) a double rotation of twenty-five degrees from the $[11\bar{2}0]$ in the rolling and transverse directions. Little preferred orientation is observed in the $(10\bar{1}1)$ pole.

As stated above, the similarity between the pole figures of the rolled powder and those of the rolled sponge indicate that the same deformation mechanisms are operating in both cases, $(0001)\langle 11\bar{2}0\rangle$ slip and $\{10\bar{1}2\}$ twinning. However, the experimental results obtained for the rolled sponge due to the larger initial grain size are not as good as those obtained for the rolled powders. The large grain size has the effect of reducing the total number of grains which will cause diffraction, thus giving poles which are representative of only a relatively few grains and may not be totally representative of the sample as a whole.

B. SUMMARY

The following results were obtained from the examination of the pole figures of cold-rolled cobalt:

1. The $(10\bar{1}1)$, (0001), and the $(10\bar{1}0)$ pole figures were constructed for various cold-rolled cobalt samples in the form of electrodeposited sheet, rolled powder strips, and annealed sponge.

2. The texture of electrodeposited cobalt is mainly $[10\bar{1}0]$ with a large spread to the $[11\bar{2}0]$ direction with random orientation of all other directions or planes in the crystals.

3. Maximum cold reduction of electrodeposited cobalt without failure was eight percent before an initial annealing treatment above the allotropic transformation temperature of 783 ^{o}F and twenty percent after the initial annealing treatment.

4. The texture of the deposited cobalt cold-rolled eight percent without annealing was almost unchanged from the "as-received" sheet. The (0001) pole showed a slight deformation texture superimposed on the "as-received" texture.

5. The texture of the electrodeposited cobalt cold-rolled twenty percent with an initial anneal above the transformation temperature can be described as a (0001) $\langle 11\bar{2}0 \rangle$ texture with a partial retention of the original

$[10\bar{1}0]$ texture.

6. The texture of cobalt powder reduced fifteen percent by cold rolling is (0001) $\langle 11\bar{2}0 \rangle$ in which the (0001) plane is rotated twenty-five degrees to the rolling direction with the $\langle 11\bar{2}0 \rangle$ rotated twenty-five degrees in the transverse direction.

7. The texture of annealed cobalt sponge reduced forty percent by cold rolling is (0001) $\langle 11\bar{2}0 \rangle$ in which the (0001) plane is rotated twenty to twenty-five degrees in the rolling direction with the $\langle 11\bar{2}0 \rangle$ rotated twenty to twenty-five degrees in the transverse direction.

8. The mechanism of deformation during cold rolling of cobalt is (0001) $[11\bar{2}0]$ slip and $\{10\bar{1}2\}$ twinning.

CHAPTER VII

THEORETICAL DISCUSSION OF THE DEFORMATION TEXTURE OF COBALT

A. TEXTURE THEORIES

Usually the analysis of textures is confined to the study of single crystals and then rationalized in terms of polycrystalline materials. Many theories have been proposed to relate polycrystalline behavior to that of single crystals, but usually oversimplified considerations have resulted.

Four main theories have been suggested to predict observed rolling textures. In 1931, Boas and Schmid (41) proposed that the three most favorably stressed slip systems are active and the orientation of such systems composing the deformation texture must be stable under the action of slip. Thus, the rotations due to slip cancel each other. This proposal was able to account for some observed tension and compression textures for several face-centered and body-centered cubic metals.

Pickers and Mathewson (42) suggested a theory of

---

(41) W. Boas and R. Schmid, "The Interpretation of the Deformation Textures of Metals", Z. Tech. Physik., Vol. 12, p. 71, 1931.

(42) M.R. Pickers and C.H. Mathewson, "On the Theory of The Origin of Rolling Textures in Face-Centered Cubic Metals", Journal Inst. of Met., Vol. 64, pp. 237-60, 1939.

rolling textures in which three or more operating slip systems lead to end positions in the texture so that the slip directions are symmetric about the direction of flow. This symmetric positioning causes the rotations to cancel each other and makes the resolved shear stresses equal. The slip systems which operate are chosen as being proportional to the product of the resolved shear stress and the cosine of the angle between the direction of flow and the slip direction. This theory successfully predicted some cold-rolled textures of face-centered cubic metals.

Taylor (43) developed a rigorous mathematical theory of deformation which was based on five operating slip systems. Five slip systems were chosen to permit any desired change in shape of the material. The choice of systems is based on the principle that the minimum number of systems will function in producing a given change in shape. This analysis can predict successfully the texture of face-centered cubic metals but is highly complex and unsatisfactory for complicated systems. For example, when the theory is applied to iron, (44) which consists of 48 slip systems, there are 1,712,304 ways to consider five possible slip systems.

---

(43) G.I. Taylor, "Mechanism of Plastic Deformation of Crystals", Proc. Royal Soc. (London), Vol. 145, pp. 362-404, 1934.

(44) C.S. Barrett, Structure of Metals, (New York: McGraw-Hill, 1952), p. 452.

In 1950 and 1951, Calnan and Clews published articles on texture analysis based on geometrical considerations. Rotations from single-slip to duplex-slip and sometimes to multiple-slip positions were considered. This theory had successfully predicted the textures of face-centered cubic, (45) body-centered cubic, (46) and hexagonal close-packed (47) structures. Thus, this theory is the only method which has been able to treat all three lattice types.

B. CALNAN AND CLEWS TEXTURE ANALYSIS

Calnan and Clews (48) (49) (50) have developed the only method of dealing with inhomogeneous deformation while explaining the deformation behavior of polycrystalline materials in comparison to the behavior of single crystals. The technique used by Calnan and Clews was a graphical

---

(45) E.A. Calnan & C.J.B. Clews, "Deformation Textures in Face-centered Cubic Metals", Phil. Mag., Vol. 41, pp. 1085-1100, 1950.

(46) E.A. Calnan & C.J.B. Clews, "The Development of Deformation Textures in Metals, Part II, Body-centered Cubic Metals", Phil. Mag., Vol. 42, pp. 616-35, 1951.

(47) E.A. Calnan & C.J.B. Clews, "The Development of Deformation Textures in Metals, Part III, Hexagonal Structures", Phil. Mag., Vol. 42, pp. 919-31, 1951.

(48) Calnan and Clews, "Face-Centered Metals", Loc. cit.

(49) Calnan and Clews, Part II, Loc. cit.

(50) Calnan and Clews, Part III, Loc. cit.

analysis of the rotations involved during slip and twinning in a single crystal.

Resolved shear stress contours are plotted in the unit stereographic triangle for each known active deformation mechanism. The resolved shear stress for slip at any point in the unit triangle is the product of the cosine of the angle of the stress axis and the slip plane normal and the cosine of the angle between the stress angle and the slip direction.

In the case of homogeneous deformation, slip must occur in more than one slip system simultaneously to prevent failure at the grain boundaries. The critical resolved shear stress, in this case, must be reached in more than one system at the same time. According to Calnan and Clews' concept, however, the effective stress can move away from the direction of the applied stress so that slip occurs at lower values of the resolved shear stress where duplex slip can sometimes occur. The movement of the effective stress is the result of constraints imposed by surrounding grains in polycrystalline material which prevent the resolved shear stress from reaching the critical value.

After construction of the resolved shear stress diagrams, slip and twinning diagrams are obtained by analysis of the resolved shear stress contours. The slip and twinning diagrams for the active systems are combined, indicating the end positions for the deformation mechanisms involved.

A more complete study of this technique was made by Williams. (51) (52)

C. DEFORMATION BY SLIP

The tension and compression slip rotations resulting from (0001) $\langle 11\bar{2}0 \rangle$, (10$\bar{1}$0) $\langle 11\bar{2}0 \rangle$, and (10$\bar{1}$1) $\langle 11\bar{2}0 \rangle$ slip in hexagonal metals (53) (54) are shown in Figures 27, 28, and 29, respectively. The (0001) $\langle 11\bar{2}0 \rangle$ and the (10$\bar{1}$0) $\langle 11\bar{2}0 \rangle$ systems are the same for all hexagonal metals, but the (10$\bar{1}$1) $\langle 11\bar{2}0 \rangle$ system changes slightly as a result of changes in the c/a ratios. When the c/a ratio change is small, the change in the (10$\bar{1}$1) $\langle 11\bar{2}0 \rangle$ slip rotations can not be plotted on a stereographic net.

In tension (0001) $\langle 11\bar{2}0 \rangle$ slip rotations result in a strong $[11\bar{2}0]$ texture with a spread toward a weak $[10\bar{1}0]$ component. However, for the (10$\bar{1}$0) $\langle 11\bar{2}0 \rangle$ and the (10$\bar{1}$1) $\langle 11\bar{2}0 \rangle$ systems in tension, the slip rotations lead to a strong $[10\bar{1}0]$ texture with a weak $[11\bar{2}0]$ component.

---

(51) D.N. Williams, "An Investigation of the Deformation Textures of Titanium", University of Missouri, Ph.D. Dissertation, (M.S.M.-T 1036), 1952.

(52) D.N. Williams & D.S. Eppelsheimer, "A Theoretical Investigation of the Deformation Texture of Titanium", Journal of Institute of Metals, Vol. 81, 1952, pp. 553-562.

(53) Williams, Loc. cit.

(54) Williams & Eppelsheimer, Loc. cit.

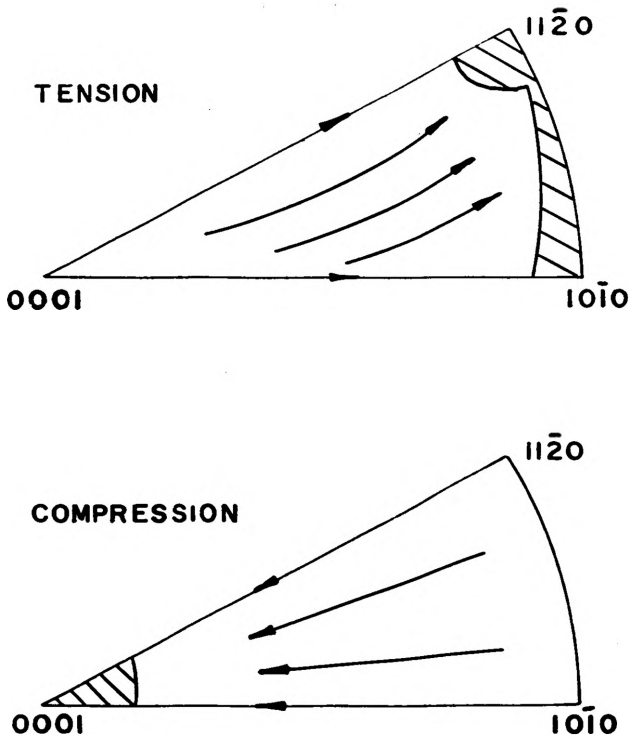

FIGURE 27. TENSION AND COMPRESSION TEXTURES RESULTING FROM $\{0001\}\langle 11\bar{2}0\rangle$ SLIP.

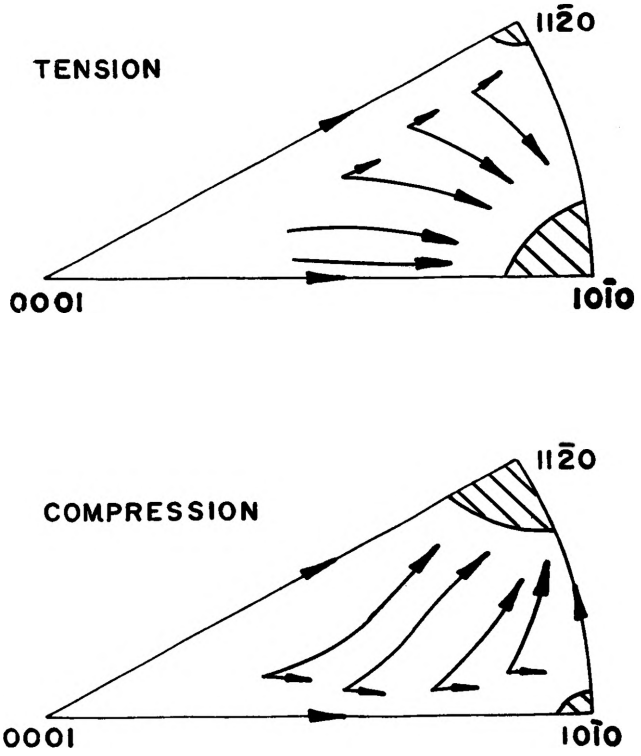

FIGURE 28. TENSION AND COMPRESSION TEXTURES RESULTING FROM $\{10\bar{1}0\}\langle 11\bar{2}0\rangle$ SLIP.

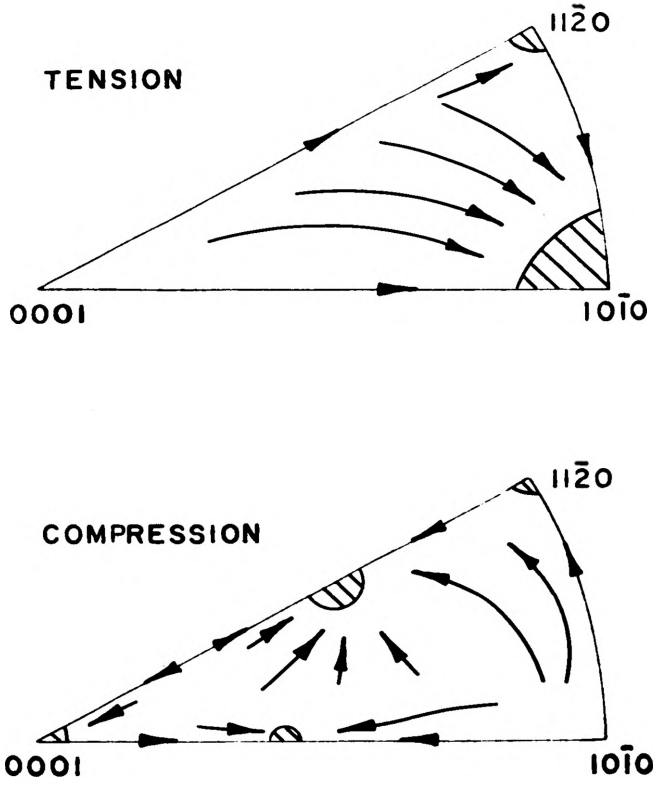

FIGURE 29. TENSION AND COMPRESSION TEXTURES RESULTING FROM $\{10\bar{1}1\}\langle 11\bar{2}0\rangle$ SLIP.

In compression, (0001) $\langle 11\bar{2}0 \rangle$ slip rotations lead to a concentration of the texture at the [0001] position. $(10\bar{1}0)$ $\langle 11\bar{2}0 \rangle$ slip rotations in compression give a strong texture in the $[11\bar{2}0]$ direction and a weak $[10\bar{1}0]$ component. However, the $(10\bar{1}1)$ $\langle 11\bar{2}0 \rangle$ in compression leads mainly to a concentration along the [0001] - $[11\bar{2}0]$ edge approximately thirty degrees from $[11\bar{2}0]$.

D. DEFORMATION BY TWINNING

In hexagonal close-packed structures two classes of twinning (55) can occur: $\{10\bar{1}2\}$ twinning and $\{11\bar{2}2\}$ or $\{11\bar{2}1\}$ twinning, which are almost the same. In tension, $\{11\bar{2}2\}$ and $\{11\bar{2}1\}$ twinning occurs near the $[11\bar{2}0]$ position of the unit stereographic triangle which tends to increase the development of a $[10\bar{1}0]$ texture. The $\{10\bar{1}2\}$ twinning, on the other hand, which occurs at the [0001] position, assists slip rotations during tension toward the $[10\bar{1}0]$ - $[11\bar{2}0]$ edge of the unit triangle.

In compression almost the reverse is true. Here $\{10\bar{1}2\}$ twinning assists slip rotations by twinning toward the [0001] position in compression. Rotations caused by $\{11\bar{2}2\}$ twinning move away from the [0001] position along the [0001] - $[11\bar{2}0]$ edge of the unit triangle.

---

(55) Williams & Eppelsheimer, Loc. cit.

E. DISCUSSION

Cold rolling is a combination of tension parallel to the rolling direction and compression normal to the rolling plane. (56) Thus, the texture expected in rolled metals with a c/a ratio close to 1.633 would be the (0001) nearly parallel to the surface. This texture is observed in magnesium.

Since the c/a ratio of cobalt (57) is 1.6228 and for magnesium (58) the ratio is 1.624, both approximately that of a system of close-packed spheres, 1.633, it can be assumed that the deformation mechanisms occurring in magnesium occur in cobalt. Twinning in magnesium (59) (60) occurs on the $(10\bar{1}2)$ plane and thus the main twinning plane in cobalt is assumed to be the $(10\bar{1}2)$.

Deformation mechanisms observed in magnesium are

---

(56) M. Cook, and T.L. Richards, "Fundamental Aspects of the Cold Working of Metals", Journal of Institute of Metals, Vol. 78, p. 463, 1951.

(57) R.T. Ananthasaman, "Lattice Parameters and Crystallographic Angles of Hexagonal Cobalt", Current Science, Vol. 27, p. 52, 1958.

(58) Cook & Richards, Loc. cit.

(59) C.S. Barrett, "The Crystallographic Mechanisms of Translation, Twinning, and Banding", Cold Working of Metals, ASM, Cleveland, 1949, p. 65.

(60) Calnan & Clews, Part III, Loc. cit.

slip on the $(10\bar{1}1)$ and the (0001) planes (61) (62) and $\{10\bar{1}2\}$ twinning. However, the $(10\bar{1}1)$ slip has only been observed above 225°C (63) or with high alloy content. (64) Because $(10\bar{1}1)$ and $(10\bar{1}0)$ slip favor a $[10\bar{1}0]$ texture and the experimental textures of cobalt show a $[11\bar{2}0]$ texture, it can be assumed that the most predominant slip system in cobalt is the $(0001)\langle 11\bar{2}0\rangle$. Because the texture of cobalt shows the (0001) plane rotated away from the rolling plane normal toward the rolling direction, the $\{10\bar{1}2\}$ twinning in tension must be great enough to cause this movement. This large amount of twinning is evident from the photomicrographs in Chapter IV. Figure 30 gives the tension and compression textures for the combined system of (0001) $\langle 11\bar{2}0\rangle$ slip and $\{10\bar{1}2\}$ twinning.

The two textures are combined in Figure 31 to form a (0001) pole figure. Compression deformation only is considered in the transverse direction while tension deformation is considered in the rolling direction. Tension and compression rotations are marked T and C in Figure 31. The resultant 0001 pole rotation is shown by the vector marked R. Twinning reorientations are denoted by the dashed arrows.

---

(61) R.L. Dietrich, "Twinning in Polycrystalline Magnesium-Discussion", Transactions AIME, Vol. 171, p. 255, 1947.

(62) Cook & Richards, Loc. cit. (63) Dietrich, Loc. cit.

(64) Cook & Richards, Loc. cit.

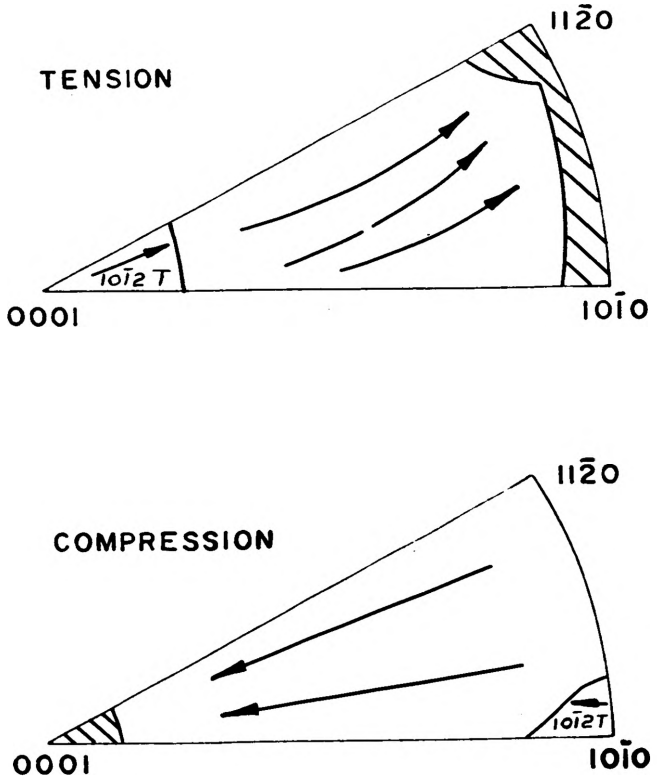

FIGURE 30. TENSION AND COMPRESSION TEXTURES RESULTING FROM (0001)<11$\bar{2}$0> SLIP AND {10$\bar{1}$2} TWINNING.

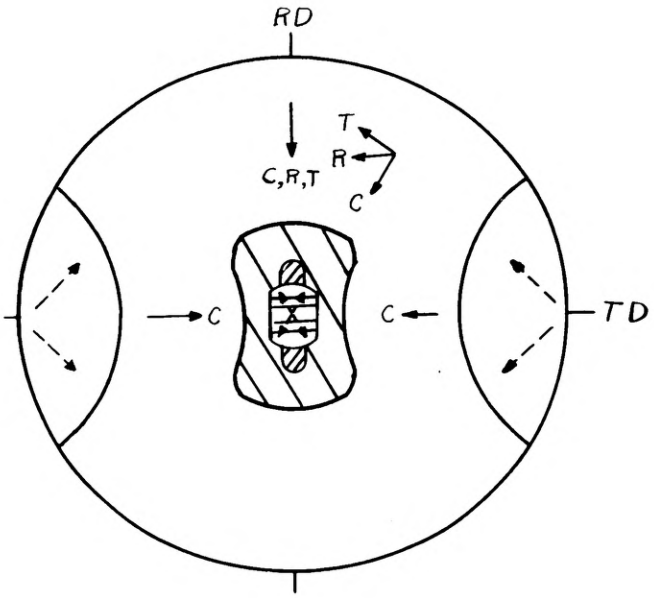

FIGURE 31. THEORETICAL (0001) POLE FIGURE OF COBALT RESULTING FROM TENSION AND COMPRESSION.

Because rotations in tension rotate the $[11\bar{2}0]$ direction in cobalt toward the rolling direction, the (0001) poles move to the rolling axis. Compression rotations move the (0001) pole toward the rolling plane normal.

The area approximately thirty degrees from the transverse direction is forbidden for (0001) poles as a result of $\{10\bar{1}2\}$ twinning in compression. These twinned poles move toward the rolling plane normal. Therefore, the area immediately around the rolling plane normal has a high concentration of (0001) poles as a result of (0001) $\langle 11\bar{2}0\rangle$ slip and $\{10\bar{1}2\}$ twinning in compression. However, the highest concentration of (0001) poles is rotated twenty degrees in the rolling direction as a result of $\{10\bar{1}2\}$ twinning in tension.

These results are partially confirmed by Wasserman, (65) who reported that the deformation texture of cobalt was very similar to that of magnesium. He also reported that the hexagonal axis of deformed cobalt was at an angle of about twenty degrees to the rolling plane normal.

The theoretical (0001) pole figure for cobalt is

---

(65) G. Wasserman, "Uber die Umwandlung des Kobalt," Metallwertschaft, Vol. 2, pp. 61-65, 1932.

somewhat different from that of magnesium (66) (67), which shows the (0001) poles concentrated at the rolling plane normal. In fact, this (0001) pole figure of cobalt is between magnesium and zinc, (68) where the (0001) poles lie in the rolling direction. The probable cause for the difference between the (0001) pole figures of magnesium and cobalt, as obtained in this report, is the difference in the amount of deformation. Usually, for texture studies, the material is cold reduced eighty to ninety-five percent. In this work, the maximum reduction obtainable was only forty percent, which is half that required for good texture studies. It would seem that twinning is the most important deformation mechanism in cobalt with relatively low reductions and thus not allowing slip to rotate the (0001) poles completely back to the rolling plane normal. Therefore, as the amount of cold reduction approaches 100 percent, slip rotations should cause the (0001) poles to concentrate more toward the center of the pole, producing a texture in cobalt more like that of magnesium.

---

(66) D.S. Gould, "An Experimental and Theoretical Investigation of the Preferred Orientation in Deformed and Recrystallized Hafnium", University of Missouri, Ph.D. Dissertation, (MSM-T1153), 1957.

(67) D.S. Eppelsheimer and D.S. Gould, "The Cold-Rolled Texture of Hafnium", Journal of Institute of Metals, Vol. 85, pp. 158-160, 1956.

(68) Gould, Loc. cit.

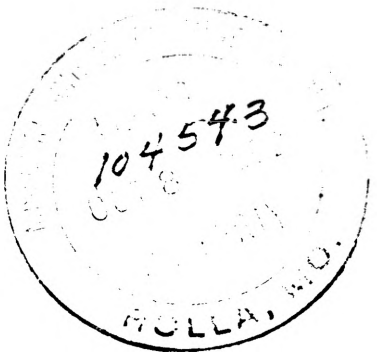

CHAPTER VIII

ANNEALING TEXTURES OF COLD-ROLLED ELECTRODEPOSITED COBALT

A search of the literature has found that no annealing textures of deformed cobalt have been reported. Because a few samples of cold-rolled electrodeposited cobalt were available, a study of the annealing textures was undertaken. Samples of the deformed cobalt were annealed at two different temperatures. At both temperatures, the samples were furnace-cooled and quenched from the annealing temperatures. One annealing temperature was below the recrystallization range and the other temperature was above this range. The electrodeposited cobalt was selected for this study because of the insufficient number of samples available from the rolled powder and the annealed sponge.

A. EXPERIMENTAL PROCEDURE

Samples of cold rolled electrodeposited cobalt having a texture such as that in Figure 16 were annealed for one hour in a vacuum at temperatures of 385°F and 720°F. Two samples were annealed at both 385°F and 720°F. Samples were both furnace-cooled and water-quenched from the annealing temperatures.

Both temperatures were below the temperature of the allotropic transformation. However, the recrystallization

range of cobalt (69) is between 570°F and 660°F. Thus, the annealing temperature of 385°F is below and the temperature of 720°F is above the recrystallization range.

The samples were pickled in concentrated HCl to remove oil from the rolls. The samples were then sealed in an evacuated pyrex tube at the annealing temperature in a pot-furnace for one hour. Those samples to be quenched were removed from the furnace and quenched in water, immediately breaking the pyrex tube. The samples to be furnace-cooled remained in the furnace over night for cooling to room temperature. The Schulz-Decker technique (Appendix II) was used to determine the texture.

The (0001) pole figures of rolled electrodeposited cobalt annealed at 385°F and 720°F are given in Figures 32 and 33.

B. DISCUSSION OF RESULTS

The $(10\bar{1}1)$, (0001), and the $(10\bar{1}0)$ pole figures were obtained for all samples involved in annealing. However, little or no difference occurred in the respective pole figures between annealing treatments below the transformation temperature, so that only the (0001) poles are reported to show this similarity.

---

(69) H. Bibring, and F. Sebilleau, "Structure et Transformation Allotropique du Cobalt", Revue De Metallugie, Vol. 52, p. 569, 1955.

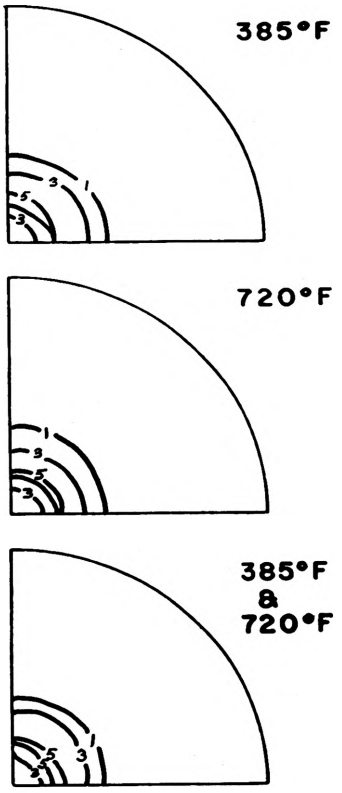

FIGURE 32. THE (0001) POLE FIGURES FOR ANNEALED AND FURNACE-COOLED ELECTRODEPOSITED COBALT REDUCED 20 PERCENT BY COLD ROLLING.

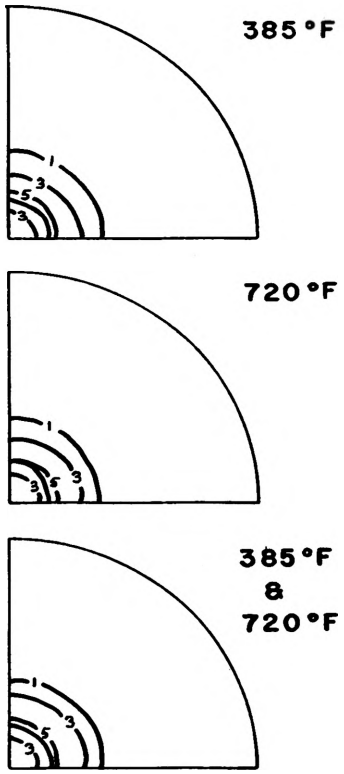

FIGURE 33. THE (0001) POLE FIGURES FOR ANNEALED AND QUENCHED ELECTRO-DEPOSITED COBALT REDUCED 20 PERCENT BY COLD ROLLING.

In all cases the maximum in the (0001) pole was rotated from the rolling plane normal in the unannealed sample to a position twenty degrees radially about the rolling plane normal. This radial maximum indicates that the (0001) plane is still somewhat in the rolling plane, but there is no defined direction aligned in the rolling direction. This indefinite alignment of a direction, as in the case of the unannealed sample, is the result of a partial retention of the "as-received" electrodeposited textures.

The $(10\bar{1}1)$ poles showed very little preferred orientation. However, in all cases, the radial maximum has been moved to forty degrees from the rolling plane normal, which is a very small change from the unannealed samples.

The greatest difference in the pole figures occurred in the $(10\bar{1}0)$ poles when comparing the furnace-cooled samples with the quenched samples. The furnace-cooled samples had a maximum in the $(10\bar{1}0)$ pole which can be described as a double rotation of twenty degrees about the $[\bar{1}2\bar{1}0]$ in both the rolling and transverse directions when annealed at 385°F. With increased temperature to 720°F or the double anneal at 385°F and then at 720°F there is a strong tendency for the maximum to spread radially about sixty-five degrees from the center of the pole. This tendency for a radial maximum sixty-five degrees from the center of the pole was also observed in the quenched structures with increasing annealing temperature. The only difference is that

the quenched sample from 385°F has a maximum rotated twenty-five degrees from the rolling direction toward the center of the pole which spreads out radially with increasing temperature. In all the $(10\bar{1}0)$ poles, a low intensity maximum was observed which was rotated thirty degrees in the rolling direction from the $(10\bar{1}0)$ position (the center of the pole).

From the above discussion, it is evident that annealed cold-rolled electrodeposited cobalt below the transformation temperature has practically no effect on the cold-rolled texture. One reason for this unaffected texture by annealing is that the initial annealing treatment before cold rolling was unable to remove completely the large columnar grains present in the "as-deposited" material, and twenty percent deformation could not introduce enough strain for complete recrystallization. The rolling direction being normal to the direction of crystal growth prevents a large amount of deformation before failure. Therefore, the texture of annealed cold-worked electrodeposited cobalt may be described as the (0001) plane approaching the rolling plane, being rotated twenty degrees from the rolling plane normal, but with both the $[11\bar{2}0]$ and the $[10\bar{1}0]$ directions aligned in the rolling direction. From these results, it is felt that these annealing textures are not truly representative of annealing textures which could be obtained with better

starting samples such as the rolled powders or the annealed sponge.

C. SUMMARY

1. The texture of cold-rolled electrodeposited cobalt after an initial anneal above the transformation temperature before rolling was determined after annealing for one hour at 385°F, 720°F and 385°F followed by one hour at 720°F. Samples were both furnace-cooled and quenched from the annealing temperature.

2. The texture obtained was a mixture of (0001) $\langle 11\bar{2}0 \rangle$ and (0001) $\langle 10\bar{1}0 \rangle$ in which the (0001) planes were rotated twenty degrees radially about the rolling plane normal.

3. The annealing texture was almost unchanged from the cold-rolled texture due to the relatively low deformation and partial retention of the "as-deposited" texture throughout all the physical operations performed on the deposited cobalt.

4. The annealing texture of rolled deposited cobalt is not representative of annealing textures which would be produced from the rolled powder or the rolled sponge due to the original crystal orientation of the deposited cobalt.

CHAPTER IX

SUMMARY AND CONCLUSIONS

A. SUMMARY

The textures of cobalt deformed by cold rolling were studied by means of the Schulz-Decker technique. Also, a study of the microhardness of cobalt was made.

The textures of electrodeposited cobalt in the "as-received" state, cold-rolled without annealing, annealed above the allotropic transformation temperature, cold-rolled after annealing, and annealed after cold rolling were studied. Samples of cold-rolled sintered cobalt powder and cold-rolled annealed sponge were examined and the textures determined. The texture as a result of different amounts of cold reduction was determined for both the rolled powder and the rolled sponge.

The deformation textures of cobalt were analyzed by the use of the Calnan and Clews texture method. This analysis was performed by considering the possible slip and twinning mechanisms occurring in cobalt. By means of the determined deformation mechanisms which occur, a theoretical (0001) pole for cold-rolled cobalt was developed.

In the short study of microhardness, the hardness was examined in terms of the structure and the amount of cold deformation. The hardness as affected by grain orientation

and twinning was also studied.

B. CONCLUSIONS

The following conclusions were developed in the investigation of the deformation textures of cobalt:

1. Microhardness varied with the source of the cobalt, the crystal orientation, and the amount of deformation and twinning. Deformation lines caused by the introduction of stress when making the hardness indentations, diffused and broadened after the hardness test indicating that some plastic flow of the deformed material occurred at room temperature.

2. The texture of electrodeposited cobalt is mainly $[10\bar{1}0]$ with a large spread to the $[11\bar{2}0]$ direction with random orientation of the grains about these directions. The texture of electrodeposited cobalt was unaffected by rolling when the rolling was performed before annealing above the allotropic transformation. After annealing above the transformation temperature, twenty percent rolling causes a texture which can be described as (0001) $\langle 11\bar{2}0 \rangle$ with a partial retention of the original $[10\bar{1}0]$ texture.

3. The annealing textures of rolled annealed electrodeposited cobalt, when the annealing temperature is below the allotropic transformation of 783°F, is a mixture of (0001) $\langle 11\bar{2}0 \rangle$ and (0001) $\langle 10\bar{1}0 \rangle$ in which the (0001) planes are rotated twenty degrees about the rolling plane normal. The annealing textures were unchanged from the cold-rolled

texture and are not representive of annealing textures which would be produced from material without an original crystal orientation.

4. The cold-rolled textures of sintered cobalt powder and annealed sponge are the same. This texture can be described as (0001) $\langle 11\bar{2}0 \rangle$ in which the (0001) planes are rotated twenty to twenty-five degrees in the rolling direction with the $\langle 11\bar{2}0 \rangle$ direction rotated twenty to twenty-five degrees in the transverse direction.

5. The cold-rolled texture of cobalt was found to be the result of (0001) $[11\bar{2}0]$ slip and $\{10\bar{1}2\}$ twinning. Slip in compression rotated the (0001) planes to the rolling plane normal while in tension the slip caused the $\langle 11\bar{2}0 \rangle$ direction to rotate toward the rolling direction. Twinning in compression assisted slip in the rotation of the (0001) planes to the rolling plane normal and, also, caused these planes to rotate away from the normal in tension.

6. The textures obtained in this investigation are representive of cobalt textures up to approximately fifty to sixty percent reduction. However, more representive textures are developed with deformation in the range of seventy-five to ninety percent reduction. With a larger amount of reduction than obtained in this investigation, the deformation textures of cobalt may approach closer to those of magnesium.

BIBLIOGRAPHY

BIBLIOGRAPHY

Anantharaman, R.T., "Lattice Parameter and Crystallographic Angles of Hexagonal Cobalt", Current Science, Vol. 27, p. 51, 1958.

Bakarian, P.W., "Preferred Orientation in Rolled Magnesium and Magnesium Alloys", Transactions AIME, Vol. 147, p. 266, 1942.

Barrett, C.S., Structure of Metals, New York: McGraw-Hill, 1952.

_____, "The Crystallographic Mechanisms of Translation, Twinning, and Banding", Cold Working of Metals, Cleveland: American Society for Metals, 1949.

Bibring, H., and F. Sebilleau, "Structure et Transformation Allotropique Du Cobalt", Revue De Metallurgie, Vol. 52, p. 569, 1955.

_____, and _____, and C. Buckle, "The Kinetics and Morphology of the Allotropic Transformation of Cobalt", Journal of the Institute of Metals, Vol. 87, p. 71, 1958.

Boas, W., and R. Schnid, "The Interpretation of the Deformation Textures of Metals", Z. Tech. Physik, Vol. 12, p. 71, 1931.

Calnan, E.A., and C.J.B. Clews, "Deformation Textures in Face-Centered Cubic Metals", Philosophical Magazine, Vol. 41, p. 1085, 1950.

_____, and _____, "The Development of Deformation Textures in Metals - Part II. Body-Centered Cubic Metals", Philosophical Magazine, Vol. 42, p. 616, 1951.

_____, and _____, "The Development of Deformation Textures in Metals - Part III. Hexagonal Structures", Philosophical Magazine, Vol. 42, p. 919, 1951.

Chernock, W.P., and P.A. Beck, "Analysis of Certain Errors in the X-Ray Reflection Method for the Quantitative Determination of Preferred Orientation", Journal of Applied Physics, Vol. 23, p. 341, 1952.

Cook, M., and T.L. Richards, "Fundamental Aspects of the Cold Working of Metals", Journal of the Institute of Metals, Vol. 78, p. 463, 1951.

Cullity, B.D., Elements of X-Ray Diffraction, Reading, Massachusetts: Addison-Wesley, 1956.

Decker, B.F., and E.T. Asp, and D. Hacker, "Preferred Orientation Determination Using a Geiger Counter X-Ray Diffraction Goniometer", Journal of Applied Physics, Vol. 19, p. 388, 1948.

Dietrich, R.L., "Twinning in Polycrystalline Magnesium - Discussion", Transactions AIME, Vol. 171, p. 255, 1947.

Eppelsheimer, D.S., and D.S. Gould, "The Cold-Rolled Texture of Hafnium", Journal of the Institute of Metals, Vol. 85, p. 158, 1956.

Gould, D.S., "An Experimental and Theoretical Investigation of the Preferred Orientation in Deformed Hafnium and Recrystallized Hafnium", U. of Mo., Ph.D. Dissertation, (M.S.M. - T1153), 1957.

Hargreave, A., "Methods of Examining Orientation Textures", X-Ray Diffraction by Polycrystalline Material, London: The Institute of Physics, 1955.

Instructions For Use of the Bergsman Micro Hardness Tester, New York: Olsen Scientific Instruments.

Klug, H.P., and L.E. Alexander, X-Ray Diffraction Procedures, New York: John Wiley and Sons, 1954.

Metals Handbook, 1948 Edition, Cleveland: American Society for Metals, 1948, p. 92.

Metallographic Etching Reagents for Cobalt and Cobalt-Containing Alloys, Columbus, Ohio: Cobalt Information Center, Battelle Memorial Institute.

Morell, L.G., and J.D. Hanawatt, "X-Ray Study of Plastic Working of Magnesium Alloys", Journal of Applied Physics, Vol. 3, p. 163, 1932.

Morral, F.R., Chronology of Cobalt, Columbus, Ohio: Battelle Memorial Institute.

_____, Cobalt and Its Alloys, Columbus, Ohio: Stoneman Press, 1958.

_____, "High-Purity Cobalt - Its Properties", Journal of Metals, Vol. 10, p. 662, 1958.

Pickers, M.R., and C.H. Mathewson, "On the Theory of the Origin of Rolling Textures in Face-Centered Cubic Metals", Journal of the Institute of Metals, Vol. 24, p. 237, 1939.

Schulz, L.G., "A Direct Method of Determining Preferred Orientation in Flat Reflection Samples Using a Geiger Counter X-Ray Spectrometer", Journal of Applied Physics, Vol. 20, p. 1030, 1949.

Taylor, G.I., "Mechanism of Plastic Deformation of Crystals", Proceeding Royal Society (London), Vol. 145, p. 362, 1934.

Wasserman, G., Textures of Metallic Materials, Berlin: Julius Springer, 1939.

_____, "Uber die Umwandlung des Kobalt", Metallwertschaft, Vol. 2, p. 61, 1932.

Williams, D.N., "An Investigation of the Deformation Texture of Titanium", U. of Mo., Ph.D. Dissertation, (M.S.M. - T1036), 1952.

_____, and D.S. Eppelsheimer, "A Theoretical Investigation of the Deformation Textures of Titanium", Journal of the Institute of Metals, Vol. 81, p. 553, 1952.

_____, and _____, "Universal Specimen Mount for Pole Figure Determination Using the Schulz-Decker Technique", Missouri School of Mines Technical Bulletin No. 79, Jan., 1952.

APPENDIX

APPENDIX I

DEFOCUSING FACTOR

Defocusing as a result of certain parts of the irradiated area of the specimen moving off the focusing circle described by the source, the specimen surface, and the receiving slit, as the specimen is revolved, causes a decrease in intensity as the angle of revolution increases from the center of the pole figure. (70) This defocusing occurs even with a randomly oriented powder and is superimposed on any texture study.

To minimize this effect, cobalt powder was run at each angle of revolution and rotation used in the texture study. The intensities for the $(10\bar{1}1)$, (0002) and the $(10\bar{1}0)$ lines were recorded and an average of three readings for each point was taken to minimize any fluctuation in the recorded intensities. The intensities at each angle of revolution were averaged and then divided into the average intensity at ninety degrees revolution, which is at the center of the pole figure. The factors thus obtained will raise the intensity at any given angle of revolution to the correct intensity. The recorded intensities and correction

---

(70) W.P. Chernock and P.A. Beck, "Analysis of Certain Errors in the X-Ray Reflection Method for the Quantitative Determination of Preferred Orientation", Journal of Applied Physics, Vol. 23, p. 341, 1952.

factors for each ten-degree angle of revolution for the $(10\bar{1}1)$, (0002) and the $(10\bar{1}0)$ lines are shown in Table VI. From examination of the correction factors for each line, it can not be assumed that the average of the defocusing correction factors for each angle of revolution involved can be used collectively for all three lines.

TABLE VI

DEFOCUSING CORRECTIONS FOR THE $(10\bar{1}1)$, (0002) AND THE $(10\bar{1}0)$ PLANES OF COBALT

(a) For Peak Height

Angle of Revolution	Correction Factor		
	$10\bar{1}1$	0002	$10\bar{1}0$
90°	1.000	1.000	1.000
80°	1.000	1.000	1.000
70°	1.020	1.045	1.027
60°	1.128	1.221	1.225
50°	1.263	1.385	1.455
40°	1.438	1.715	1.840
30°	2.080	2.280	2.550

(b) For Peak Area

Angle of Revolution	Correction Factor		
	$10\bar{1}1$	0002	$10\bar{1}0$
90°	1.000	1.000	1.000
80°	1.000	1.000	1.000
70°	1.012	1.012	1.000
60°	1.079	1.057	1.035
50°	1.085	1.100	1.050
40°	1.142	1.113	1.122
30°	1.205	1.153	1.190

APPENDIX II

X-RAY TECHNIQUE

A universal specimen mount constructed by Williams (71) (72) at the Missouri School of Mines in connection with a Norelco X-ray unit was used for the determination of the pole figures for all sheet materials. This mount enabled the entire pole figure to be constructed after correcting the intensity readings for defocusing and absorption.

Intensity readings were taken by running the Geiger counter over twelve to fifteen degrees to cover the correct value of 2 θ of all three diffracted lines after each movement of the sample. An average of three readings was used to minimize any fluctuation of intensity. Thus, more consistent results were obtained. Intensities were measured either by the height of the peak above background or the area contained by the peak. The difference in results obtained by measuring the intensities by these two methods is discussed in Part A of this Appendix.

---

(71) D.N. Williams and D.S. Eppelsheimer, "Universal Specimen Mount for Pole Figure Determination using the Schulz-Decker Technique", University of Missouri, School of Mines and Metallurgy, Bulletin No. 79, 1952.

(72) D.N. Williams, "An Investigation of the Deformation Texture of Titanium", University of Missouri, Ph.D. Dissertation, (M.S.M.-T1036), 1952.

The data obtained from the intensity readings were plotted directly on a polar stereographic net. Examination of the intensities at the thirty-degree latitude circle obtained by both transmission and reflection enables the necessary correction to be made between the two methods to make their intensities equal. The transmission readings were then corrected to correspond to the reflection readings. Figure 34 illustrates a typical portion of the recorded intensities for the forty percent rolled sponge.

The centering of the sample was performed by mounting the sample and measuring the intensity at 0, 30, 60, and 90 degrees rotation at the center of the pole. The sample was continuously remounted until all recorded intensities for each angle of rotation at the center of the pole were equal. When all recorded intensities at the pole center were the same, the sample was considered to be centered correctly.

After the sample was centered, the selection of the correct slit system had to be made to prevent the recorded intensities from either being too low to be read or from being too high and thus not recording the entire peak. Only vertical slits were used at the X-ray tube and the Geiger counter. The vertical slit at the Geiger counter allowed better resolution of the $(10\bar{1}1)$ and (0002) reflections than a horizontal slit.

The vertical slit at the X-ray tube was used in

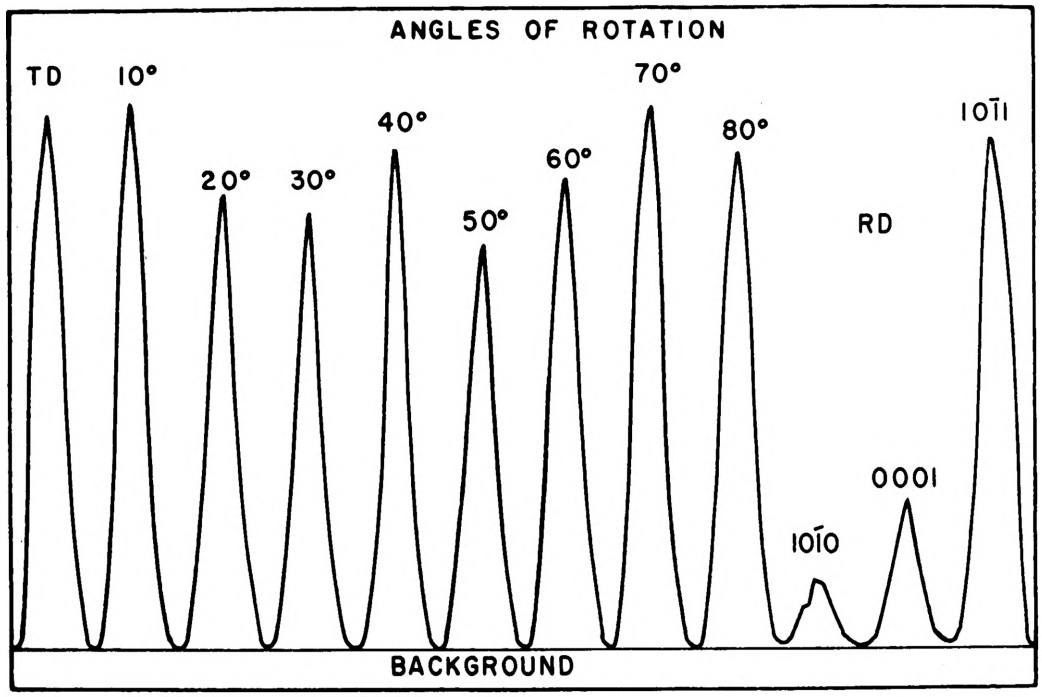

FIGURE 34. RECORDED $10\bar{1}1$ REFLECTION INTENSITIES AT 50° REVOLUTION FOR 40 PERCENT COLD-ROLLED SPONGE.

combination with a horizontal slit mounted on the specimen mount. This combination of horizontal and vertical slits permitted a square beam to hit the center of the specimen surface. This square beam permitted the use of a rectangular specimen. If only a vertical or horizontal slit was used between the X-ray tube and the sample without the aid of the other slit, a circular sample must be used. The use of one slit would allow the X-ray beam to hit across the center of the entire sample and as the sample was rotated, the area of reflection of a rectangular sample would change, causing an error in the recorded intensities. However, with the use of the double-slit system on the primary X-ray beam, this error in the recorded intensities resulting from changing area could not occur.

A. DIFFERENCE IN INTENSITY MEASUREMENTS

Considerable thought was given to the correct method of measuring the intensities obtained in this work. Two methods were used to determine which one was best or if both could be used. These methods were the measurement of the peak height above background and the measurement of the peak area by the use of a compensating polar planimeter. In connection with these two methods, the three main hexagonal close-packed lines, the $(10\bar{1}1)$, the $(10\bar{1}0)$ and the (0002) of the forty percent cold-reduced vacuum-melted and

annealed sponge were used. The comparison was performed on both the reflection and transmission samples covering the entire pole figure.

Figures 35 through 37 illustrate the results of measuring the intensity by both methods after making absorption and defocusing corrections. It is seen in these figures that there is very little or no difference obtained by the use of the two methods for the measurement of the intensities.

The pole for the $(10\bar{1}1)$ line (Figure 35) in both cases shows a maximum at approximately forty degrees from the transverse direction. The only difference in the poles is the size of the maximum which is larger in the pole figure obtained by relative height. For the $(10\bar{1}0)$ pole (Figure 36) the contour lines are almost concentric around the center of the pole figure. The maximum is at thirty degrees revolution and sixty degrees rotation toward the rolling direction.

It would seem that perhaps the greatest difference is in the (0002) pole, (Figure 37). In this case, the maximum for both is at seventy-five degrees revolution from the rolling direction. However, the maximum resulting from the peak height is much larger than the one resulting from the area and extends to the center of the pole. However, if a larger maximum number had been chosen for peak height, the poles produced by both methods would have been

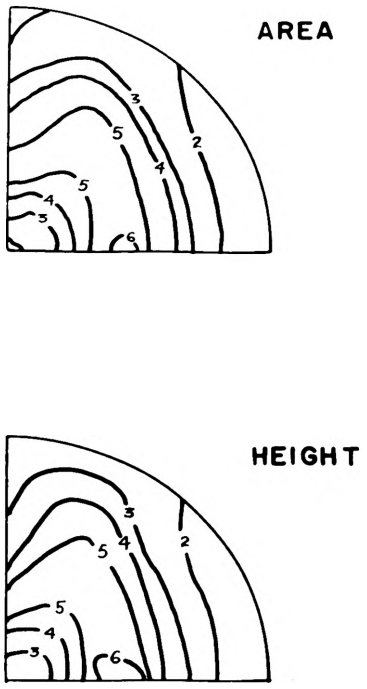

FIGURE 35. THE (10$\bar{1}$1) POLE FIGURE FOR 40 PERCENT COLD-ROLLED SPONGE OBTAINED BY MEASUREMENT OF PEAK AREA AND PEAK HEIGHT.

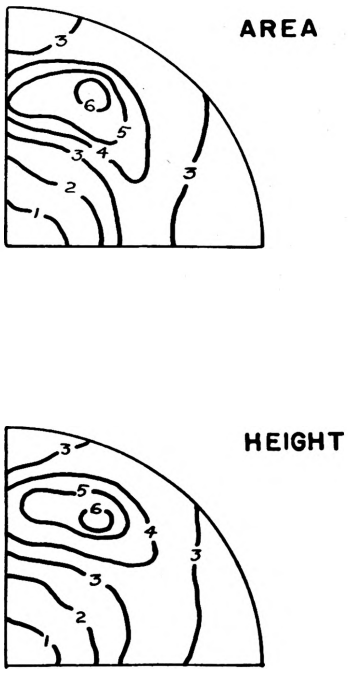

FIGURE 36. THE $(10\bar{1}0)$ POLE FIGURE FOR 40 PERCENT COLD-ROLLED SPONGE OBTAINED BY MEASUREMENT OF PEAK AREA AND PEAK HEIGHT.

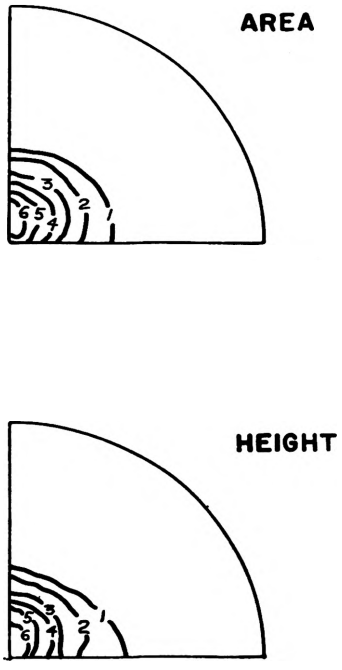

FIGURE 37. THE (0001) POLE FIGURE FOR 40 PERCENT COLD-ROLLED SPONGE OBTAINED BY MEASUREMENT OF PEAK AREA AND PEAK HEIGHT.

the same.

Thus, from the inspection of the pole figures discussed, it is apparent that either of the two methods, peak height or area, can be used for the measurement of the intensity. This is because relative intensity and not integrated intensity is used. However, it must be remembered that the intensities measured by both methods must be corrected for defocusing.

B. TABULATION OF INTENSITY DATA

Tables VII and VIII list the recorded intensities of the $(10\bar{1}0)$ pole figure for forty percent cold-rolled annealed sponge cobalt. The transmission readings must be corrected for absorption, and the reflection reading obtained by peak area must be corrected for defocusing before the two sets can be correlated.

The Decker absorption formula and the method of determining μt was used for the absorption corrections of the transmission reading. (73) The intensity of the (110) alpha brass line was measured with the counter open and then again with the cobalt transmission sample in the diffracted beam. These intensities are I_o and I_t, respectively, and

---

(73) B.F. Decker, E.T. Asp and D. Harker, "Preferred Orientation Determination Using a Geiger Counter X-Ray Diffraction Gonometer", Journal of Applied Physics, Vol. 19, 1948, pp. 388-92.

TABLE VII

RECORDED REFLECTION INTENSITIES OF THE $(10\bar{1}0)$ PLANE FOR 40 PERCENT COLD REDUCED ANNEALED SPONGE COBALT

Angle of Revolution	Angle of Rotation									
	TD	10°	20°	30°	40°	50°	60°	70°	80°	RD
90°	7			7			7			7
80°	9			7			10			6
70°	8	9	9	7	12	12	14	15	12	12
60°	14	19	19	15	19	20	18	18	18	17
50°	23	22	23	20	25	26	26	25	25	22
40°	34	33	33	31	31	34	31	31	48	34
30°	38	42	32	43	38	43	37	49	59	53

TABLE VIII

RECORDED TRANSMISSION INTENSITIES OF THE $(10\bar{1}0)$ PLANE FOR 40 PERCENT COLD REDUCED ANNEALED SPONGE COBALT

Angle of Revolution	Angle of Rotation									
	TD	10°	20°	30°	40°	50°	60°	70°	80°	RD
30°	23	24	26	35	44	53	52	46	44	43
20°	32	37	46	43	59	71	95	77	64	55
10°	48	56	50	62	67	64	78	64	54	52
0°	56	54	49	68	65	78	74	73	54	46

are used to calculate μ. This calculation was performed as follows:

$$I_o = 1880$$
$$I_t = 50$$
$$\mu t = \ln I_o/I_t$$
$$\mu t = 5.75$$

The correction factors necessary for the $(10\bar{1}0)$ line are given in Table IX. The corrected transmission readings were found by multiplying the recorded intensity by the correction factor. The corrected transmission intensities are given in Table X.

Before correlating the corrected transmission intensities with the reflection intensities, the reflection reading must be corrected for defocusing to prevent superimposing the effects of defocusing on the pole figure. The defocusing correction factors listed in Table VI were used to make this correction. The recorded reflection readings were multiplied by the above defocusing factors to obtain the corrected reflection intensities, which are given in Table XI.

After correcting the transmission intensities for absorption and the reflection for defocusing, the corrected intensities were correlated. The intensities at thirty degrees were used for the correlation. The transmission intensities at thirty degrees were divided into the reflection intensities. The values thus obtained were averaged, giving a factor of 0.502. All transmission intensities were

TABLE IX

ABSORPTION CORRECTION FORMULA AND CORRECTION FACTORS FOR THE $(10\bar{1}0)$ PLANE*

Angle of Revolution	Correction Factor
30°	2.740
20°	1.630
10°	1.185
0°	1.000

*The absorption equation in Chapter II under the Diffractometer Method was reduced for cobalt, only, to the following form:

$$I_o/I_{\pm\alpha} = \frac{A\,\mu t\,(e^{-\mu t})^B}{(e^{-\mu t})^C - (e^{-\mu t})^D} \qquad (6)$$

where the constants depend on the Bragg angle, θ, for an individual line and these constants are given below:

		A	B	C	D
$10\bar{1}1$					
	10°	0.267	1.159	1.068	1.315
	20°	0.626	1.159	1.107	1.568
	30°	1.183	1.159	1.000	2.020
0001					
	10°	0.239	1.136	1.055	1.277
	20°	0.557	1.136	1.010	1.505
	30°	1.033	1.136	1.000	1.908
$10\bar{1}0$					
	10°	0.212	1.115	1.042	1.245
	20°	0.492	1.115	1.008	1.449
	30°	0.893	1.115	1.002	1.805

TABLE X

CORRECTED TRANSMISSION INTENSITIES

Angle of Revolution	Angle of Rotation									
	TD	10°	20°	30°	40°	50°	60°	70°	80°	RD
30°	63	66	71	96	120	145	142	126	120	118
20°	52	60	75	70	96	116	155	126	104	90
10°	56	66	59	73	79	75	92	75	63	61
0°	56	54	49	68	65	78	74	73	54	46

TABLE XI

REFLECTION INTENSITIES CORRECTED FOR DEFOCUSING

Angle of Revolution	Angle of Rotation									
	TD	10°	20°	30°	40°	50°	60°	70°	80°	RD
90°	7			7			7			7
80°	9			7			10			6
70°	8	9	9	7	12	12	14	15	12	12
60°	15	20	20	16	20	21	19	19	19	18
50°	24	23	24	21	26	27	27	26	26	23
40°	38	37	37	34	34	38	34	34	53	38
30°	45	50	38	51	45	51	44	58	70	63

TABLE XII

COMBINED CORRECTED INTENSITIES

Angle of Revolution	Angle of Rotation TD	10°	20°	30°	40°	50°	60°	70°	80°	RD
90°	7			7			7			7
80°	9			7			10			6
70°	8	9	9	7	12	12	14	15	12	12
60°	15	20	20	16	20	21	19	19	19	18
50°	24	23	24	21	26	27	27	26	26	23
40°	38	37	37	34	34	38	34	34	53	38
30°	38	42	37	50	53	62	58	61	65	61
20°	26	30	38	35	48	58	78	63	52	45
10°	28	33	30	37	40	38	46	38	32	31
0°	28	27	25	34	33	39	37	37	27	23

TABLE XIII

FINAL ADJUSTED INTENSITIES

Angle of Revolution	Angle of Rotation									
	TD	10°	20°	30°	40°	50°	60°	70°	80°	RD
90°	7			7			7			7
80°	8			7			9			5
70°	7	8	8	7	11	11	12	13	11	11
60°	13	17	17	14	17	18	17	17	17	16
50°	21	20	21	18	23	24	24	23	23	20
40°	33	32	32	32	30	33	30	30	46	33
30°	33	37	32	44	46	54	51	53	57	53
20°	23	26	33	31	42	51	68	55	56	39
10°	24	29	26	32	35	33	40	33	28	27
0°	24	24	22	30	29	34	32	32	24	20

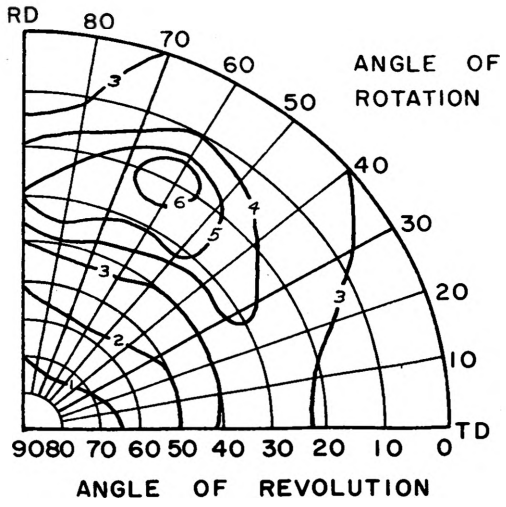

FIGURE 38. THE $(10\bar{1}0)$ POLE FIGURE OF 40 PERCENT COLD-ROLLED SPONGE WITH ANGLES OF REVOLUTION AND ROTATION INDICATED.

then multiplied by this factor to make them correspond to the reflection intensities. The combined intensities at thirty degrees were obtained by taking the mean values of the transmission and reflection readings after correction. The combined correlated intensities are given in Table XII.

C. PLOTTING OF DATA

The maximum intensity in Table XII was reduced to a value of 70 units. This was done for convenience in plotting. The intensity was reduced by multiplying all the values by the ratio of the maximum value to a maximum arbitrary value, 80/70. Table XIII lists the final adjusted intensity values.

The pole figure was constructed by plotting each intensity value on its particular angles of revolution and rotation on a polar stereographic net. Contour lines were then drawn connecting constant intensity values. The pole figure for the above data is given in Figure 38 with the angles of revolution and rotation indicated.

APPENDIX III

PROCEDURE FOR OPERATING THE BERGSMAN MICRO HARDNESS TESTER

The Bergsman Micro Hardness Tester manufactured by Olsen Scientific Instruments consists mainly of an indicator arm for alignment of the load over the indentor and a base plate for holding the sample. (74) The tester is mounted directly on the stage of a metallograph after all detachable parts on the stage have been removed. The procedure for the operation of the tester is subdivided into the following operations.

Adjustment of Indicator Arm. The indicator arm with its mount should be placed behind the main portion of the metallograph to prevent moving the indicator while making the hardness tests. The indicator arm is positioned so that the point is approximately over the center of the objective lens and about two to three inches above the lowered stage of the metallograph. A piece of paper through which a small hole has been made is placed on the stage. The stage is then lowered until it is almost at the same level as the top of the objective lens. This position of the stage will produce the smallest beam of light on the paper that is possible.

---

(74) Instruction for use of the Bergsman Micro Hardness Tester, (New York: Olsen Scientific Instruments).

The paper is then adjusted until the center of the hole coincides with the center of the beam of light from the objective.

After adjustment of the paper to the objective, the stage is raised until it is just below the pointer of the indicator arm. The pointer is then adjusted to coincide with the hole in the paper. This positioning of the indicator arm aligns the pointer over the center of the objective or over the indentor during the hardness tests. The indicator arm is then rotated out of position to prevent movement during mounting of the base plate.

Mounting and Balancing of Tester. All detachable parts on the stage of the metallograph must be removed in order to mount the tester to the stage. The base-plate of the tester is fixed to the stage by means of a screw in the hole intended for the stage clamp.

A specimen which has been mounted in a one and a quarter inch diameter bakelite mount about one centimeter in thickness is placed in the specimen holder on the balancing arm of the tester. The specimen is held by means of a bayonet joint filling containing a screw to firmly hold the sample in place. The weight disc is mounted on top of the arrangement and fits securely in the sample holder.

After the specimen is fixed, the attachment is balanced by means of the movable counter weight at the opposite

end of the balance arm from the sample. The counter weight is adjusted by a wheel until the light on the base-plate flickers when the stage is tapped. The attachment is now ready for use. However, the above procedure is repeated with each individual sample.

Vickers Test. After the attachment is balanced, it is ready for making hardness indentations. An appropriate weight is placed on the weight disc to hold the balance arm and sample in position. A suitable objective lens is inserted in the metallograph to select the area for the hardness test. Usually, the 21X objective will be appropriate, since this allows enough magnification to select individual grains for the test. The area for testing is selected, and the stage is raised so that the weight is just below the pointer of the indicator arm. The weight is then centered under the pointer, placing the weight directly over the indentor. With the stage raised, the objective lens is replaced by the diamond indentor.

The stage is lowered until the indentor approaches the specimen. The sample is then brought into contact with the indentor by means of the fine adjustment of the metallograph. The movement of the stage is stopped immediately upon contact, when the indicator light is extinguished. The load remains on the sample for fifteen to twenty seconds, at which time the stage is raised. This removes the load and

allows replacement of the indentor by the objective lens. For the determination of the hardness, both diagonals of the indentation are measured by means of an eyepiece screw micrometer.

Several precautions must be observed while making the hardness test. The first one is that the center of gravity of the weight must be placed immediately below the pointer of the indicator arm for each indentation, since a movement of the specimen without centering the weight changes the load. Also the speed of loading must be kept constant between readings. Finally the micrometer eyepiece must be calibrated by comparison with a stage micrometer. This calibration must be made for each objective lens.

APPENDIX IV

METALLOGRAPHY OF COBALT

The metallography of cobalt presented a number of problems not only in polishing but also in etching. Scratches produced during polishing (dry or wet) were next to impossible to remove without a relatively deep etch followed by repolishing. Also, cobalt was found to be relatively unaffected by most chemical etchants or was stained badly, rendering the etchant useless. Only concentrated nitric acid was found to chemically etch cobalt to any extent, but the reaction could not be controlled, resulting in a badly corroded and heavily stained specimen.

As a result of the difficulties stated above, the following procedure was developed, which allowed the preparation of cobalt specimens for metallography in approximately two hours. After mounting, the samples were ground with a power grinder using a 320 grit belt. The specimens were then dry polished with 0 through 000 emery papers using the usual polishing techniques of rotating the sample ninety degrees after each paper. After dry grinding, a wet grind using 600 grit Buehler paper was utilized. Great care had to be used, to be sure that all scratches from preceding papers were removed before changing emery papers, as these scratches would greatly increase the time of wet polishing.

After the wet polish using 600 grit paper, final polishing was done on a cloth polishing wheel. The cloth used for the final polish was AB Metcloth. This polishing was performed with a "Linde B" abrasive. All scratches from the 600 paper could be removed in this step, but the time required was excessive. Therefore, polishing was only carried out to the extent that the majority of the scratches are removed. At this point, a heavy etch with concentrated nitric acid was given to the specimens. This was done by putting a drop of the acid on the surface of the sample and immediately washing with water. The etch is repeated two or three times depending on the depth of scratches in the sample. The sample was then returned to the polishing wheel to remove the effects of the nitric acid etch and eliminate all scratches.

To remove smearing as a result of mechanical polishing, the samples at this stage were etched electrolytically and then repolished and etched. Electrolytic etching was performed using a stainless steel wire mesh screen as the cathode with an electrolyte (75) of 60 parts HCl, 15 parts HNO_3, and 15 parts of H_2O. The cell operated at 2 volts at room temperature. The electrolyte is aged for fifteen minutes before using. After etching, the samples were

---

(75) Metallographic Etching Reagents for Cobalt and Cobalt-Containing Alloys, (Columbus, Ohio, Cobalt Information Center, Battelle Memorial Institute).

returned to the final polishing wheel to remove the effects of the anodic etch.

The final etch for metallography was carried out in the same cell described above. The time of etching varied with the structure but in all cases was a matter of only a few seconds. However, great care had to be used, because a soluble green cobalt film was deposited on the surface, making thorough washing of the specimen necessary to reduce staining.

The etching operation must be carried out in a well ventilated room due to the chloride fumes produced by the electrolyte. Also, due to the strong chemical action between the electrolyte and the stainless steel mesh in a relatively short period of time, the mesh must be removed after each operation of the cell to prevent the electrolyte from boiling over. Due to this chemical action, the electrolyte can only be used for about three or four etchings. This electrolyte can also be used for chemical etching of cobalt but heavy staining results, which reduces the desired effects.

APPENDIX V

FUTURE WORK

Future work should be directed toward obtaining a more complete picture of the deformation process which occurs in cobalt. Experiments should be designed to determine more accurately and completely the effects of the c/a ratio of cobalt on the deformation process. It is suggested that this work include the following specific items. Thus valuable information can be obtained on the deformation process of cobalt.

1. In future work, an automatic pole figure device should be used. This device is not necessary but would decrease the time required for plotting the necessary pole figures and would allow more work to be done with greater efficiency.

2. In any future study of the deformation textures of cobalt or other hexagonal close-packed metals, a finer grain material should be utilized than was obtainable in the present work. The finer the grain size of the material, the more representative the intensity of the X-ray reflections will be for the entire sample.

3. The study of the deformation textures of cobalt as a result of rolling should be extended to include samples with greater amounts of reduction than were used in this work. One way in which greater amounts of reduction might be

obtained is by warm rolling. This warm rolling could be accomplished by annealing at some temperature, making a few passes through the rolls, and then re-annealing. This process could be repeated until the proper reduction was obtained. The annealing for warm rolling should be below 300°C because the recrystallization range for cobalt is between 300°C and 350°C.

4. The study of the deformation textures of cobalt in this paper was confined mainly to rolling textures. Thus, for a more complete analysis of the preferred orientation effects in cobalt, the deformation texture study should be extended to include compression textures. Compression textures would allow further investigation of the effect of the c/a ratio of cobalt on preferred orientation compared with other hexagonal close-packed metals with different c/a ratios in which the compression textures are known.

5. In a complete study of the annealing textures of cobalt, the sponge type material should be used instead of the electrodeposited material. The original "as-deposited" texture of the electrodeposited sheets was retained throughout all rolling and annealing processes and proved to be detrimental to the study of annealing textures. With sponge material, this retention of the original texture would be eliminated because of the random orientation of the "as-received" sponge material.

VITA

The author was born in Alexandria, Virginia, on February 4, 1933. He attended public school in Alexandria until June, 1950. He was admitted to Mars Hill College in September, 1950, Virginia Polytechnic Institute in June, 1951 and received the Bachelor of Science Degree in Metallurgical Engineering in June, 1955. He worked for the Naval Ordnance Laboratory, Silver Spring, Maryland until June, 1956 at which time he entered the Army for six months. He returned to Virginia Polytechnic Institute in December, 1956 when he was appointed Instructor in the Metallurgical Engineering Department. Here, he received the Master of Science Degree in Metallurgical Engineering in June, 1959. He was admitted to the Missouri School of Mines and Metallurgy in September, 1959 and returned to Virginia Polytechnic Institute in January, 1962 as an assistant professor.

He is a member of the American Society for Metals, American Institute of Mining and Metallurgy, The British Institute of Metals, Sigma Gamma Epsilon, Alpha Sigma Mu, and Sigma Xi, and is a First Lieutenant in the Virginia National Guard.

Troy C. Wiecy